Cellular Microbiology (2014) **16**(5), 709–733

doi:10.1111/cmi.12288
First published online 4 April 2014

Perforin-like protein PPLP2 permeabilizes the red blood cell membrane during egress of *Plasmodium falciparum* gametocytes

Christine C. Wirth,[1] Svetlana Glushakova,[2] Matthias Scheuermayer,[3] Urska Repnik,[4] Swati Garg,[5] Dominik Schaack,[6] Marika M. Kachman,[2] Tim Weißbach,[1] Joshua Zimmerberg,[2] Thomas Dandekar,[6] Gareth Griffiths,[4] Chetan E. Chitnis,[5] Shailja Singh,[5,7] Rainer Fischer[1,8] and Gabriele Pradel[1,8]*

[1]*Institute of Molecular Biotechnology, RWTH Aachen University, Worringerweg 1, 52074 Aachen, Germany.*
[2]*Program in Physical Biology, Eunice Kennedy Schriver National Institute of Child Health and Human Development, National Institutes of Health, Bethesda, MD 20892, USA.*
[3]*Research Center for Infectious Diseases, University of Würzburg, Josef-Schneider-Str. 2/D15, 97080 Würzburg, Germany.*
[4]*Department of Biosciences, University of Oslo, Blindernveien 31, PO Box 1066, 0316 Oslo, Norway.*
[5]*Malaria Group, International Centre for Genetic Engineering and Biotechnology (ICGEB), Aruna Asaf Ali Marg, New Delhi 110067, India.*
[6]*Department of Bioinformatics, University of Würzburg, Am Hubland, 97074 Würzburg, Germany.*
[7]*Department of Life Sciences, Shiv Nadar University, Village Chithera, Tehsil Dadri, Gautam Budh Nagar 203207, India.*
[8]*Fraunhofer Institute of Molecular Biology and Applied Ecology, Forckenbeckstraße 6, 50274 Aachen, Germany.*

Summary

Egress of malaria parasites from the host cell requires the concerted rupture of its enveloping membranes. Hence, we investigated the role of the plasmodial perforin-like protein PPLP2 in the egress of *Plasmodium falciparum* from erythrocytes. PPLP2 is expressed in blood stage schizonts and mature gametocytes. The protein localizes in vesicular structures, which in activated gametocytes discharge PPLP2 in a calcium-dependent manner. PPLP2 comprises a MACPF domain and recombinant PPLP2 has haemolytic activities towards erythrocytes. PPLP2-deficient [PPLP2(–)] merozoites show normal egress dynamics during the erythrocytic replication cycle, but activated PPLP2(–) gametocytes were unable to leave erythrocytes and stayed trapped within these cells. While the parasitophorous vacuole membrane ruptured normally, the activated PPLP2(–) gametocytes were unable to permeabilize the erythrocyte membrane and to release the erythrocyte cytoplasm. In consequence, transmission of PPLP2(–) parasites to the *Anopheles* vector was reduced. Pore-forming equinatoxin II rescued both PPLP2(–) gametocyte exflagellation and parasite transmission. The pore sealant Tetronic 90R4, on the other hand, caused trapping of activated wild-type gametocytes within the enveloping erythrocytes, thus mimicking the PPLP2(–) loss-of-function phenotype. We propose that the haemolytic activity of PPLP2 is essential for gametocyte egress due to permeabilization of the erythrocyte membrane and depletion of the erythrocyte cytoplasm.

Received 19 December, 2013; revised 17 February, 2014; accepted 21 February, 2014. *For correspondence. E-mail gabriele.pradel@molbiotech.rwth-aachen.de; Tel. (+49) 241 8028123; Fax (+49) 241 871062.

Introduction

The perforation of target cell membranes by pore-forming proteins is a common feature of pathogenicity and immune defence. Pore-forming proteins possess the ability to switch between a soluble and a membrane-inserted pore form. In Gram-positive bacteria they are important toxins, termed cholesterol-dependent cytolysins (CDCs), which are involved in host cell invasion. In eukaryotes, the pore-forming proteins are merged within the membrane attack complex/perforin (MACPF) superfamily, originally named after a domain common to the complement proteins of the terminal membrane attack complex (MAC) and to the cytolytic protein perforin-1 (PF1) expressed by cytotoxic T lymphocytes and natural killer cells. To date, more than 500 MACPF proteins have been identified, particularly in vertebrates, but also in

plants and in the venom of sea anemones and urchins (reviewed in Rosado *et al*., 2008; Dunstone and Tweten, 2012).

Members of the MACPF proteins are also encoded by Apicomplexan parasites, including the genera *Toxoplasma*, *Eimeria*, *Theileria* and *Plasmodium*. Apicomplexan parasites are obligate intracellular parasites that invade their host cells actively and reside within a membrane-bound vacuole for the most part of their life cycle (reviewed in Baum *et al*., 2008). The presence of MACPF proteins was thus originally attributed to the parasites' ability to manipulate the host cell membranes during these processes (reviewed in Kafsack and Carruthers, 2010).

Five MACPF proteins were identified in *Plasmodium* parasites, termed plasmodial perforin-like proteins PPLP1–5 (Kaiser *et al*., 2004), and the functions of some of these proteins were subsequently studied in the rodent model parasite *P. berghei* (reviewed in Roiko and Carruthers, 2009; Kafsack and Carruthers, 2010). It was shown that the perforins PPLP3/MAOP and PPLP5 participate in the traversal of the midgut epithelium by the ookinete (Kadota *et al*., 2004; Ecker *et al*., 2007), while PPLP1/SPECT2 supports sporozoite breaching of the liver sinusoidal cell layer prior to hepatocyte invasion (Ishino *et al*., 2005). Thus, the three perforins play crucial roles for the invasion machinery of the malaria parasite by opening the host cell membranes prior to cell traversal.

Two recent studies demonstrated that the PPLPs are also involved in the egress of *Plasmodium* from its host erythrocyte. *Plasmodium* is known to egress from the red blood cell (RBC) via an inside-out mode, during which the parasitophorous vacuole membrane (PVM) ruptures prior to the erythrocyte membrane (EM) (reviewed in Wirth and Pradel, 2012). Deligianni *et al.* (2013) showed that the *P. berghei* perforin PPLP2 is important for exflagellation of male gametocytes (microgametocytes). Activated microgametocytes that lack PPLP2 were trapped within the erythrocyte, which leads to impaired transmission of these parasites to the mosquitoes. Further, Garg *et al.* (2013) reported that PPLP1 and PPLP2 are expressed in the asexual blood stages of the human malaria parasite *P. falciparum*. PPLP1 is present in the micronemes and relocalizes to the enveloping membranes of the mature schizont after being discharged in a calcium-dependent manner. Furthermore, recombinant PPLP1 exhibits membranolytic activities towards erythrocytes, indicating that this perforin may be involved in EM breakdown during merozoite egress (Garg *et al*., 2013).

In this study we aimed to investigate the role of *P. falciparum* PPLP2 in the egress behaviour of blood stage merozoites and activated gametocytes using a newly generated PPLP2-deficient [PPLP2(–)] parasite line. We showed that this perforin is dispensable for the asexual blood cycle, but crucial for the egress of activated gametocytes from the host erythrocytes due to its membranolytic activities.

Results

The MACPF protein PPLP2 is expressed in P. falciparum *blood stage parasites and gametocytes*

The *P. falciparum* gene *pplp2* (PlasmoDB gene-ID: PF3D7_1216700) encodes for a 125 kDa protein, which comprises an N-terminal signal peptide and a central MACPF domain (Fig. 1A). We aimed to determine the 3D-structure of PPLP2 using homology-modelling. Only the MACPF domain of PPLP2 but not the N- and C-terminal parts of the protein could be modelled using homology predictions of various known MACPF proteins. To model the N- and the C-terminal regions of PPLP2, AnDOM algorithm, two threading algorithms, multiple alignment secondary structure predictions and critically-reject-bad-structure predictions were used in the QUARK program (Xu and Zhang, 2012). The structural analyses resulted in the surface model of PPLP2 shown in Fig. 1B. The MACPF domain (in orange) forms a loop protruding from the globular protein. In the N-terminus (grey, left side from the central MACPF domain) a beta-sheet, two helices packed against the beta-sheet, and several coiled regions were predicted, while a globular helical region was predicted in the C-terminus. The N- and C-terminus predictions were validated by energy refinement and protein structure checks and were selected from a panel of predictions as the best quality predictions.

We investigated transcript expression of *pplp2* in the *P. falciparum* blood stages by diagnostic RT-PCR. The RNA was isolated from trophozoites, schizonts, immature gametocytes and mature gametocytes and corresponding cDNA was prepared. Diagnostic RT-PCR demonstrated transcript expression of *pplp2* in trophozoites and schizonts (Fig. 1C). Transcript was also detected in immature (stage II-IV) gametocyte samples as well as in mature (stage V) gametocytes, albeit in a lower level of expression than in stages II-IV. Amplification of transcripts for the blood stage-specific gene *ama1* (gene encoding the apical membrane protein 1; Peterson *et al*., 1989) and for the gametocyte-specific gene *pfccp2* (gene encoding for the LCCL-domain protein 2; Pradel *et al*., 2004) were used to demonstrate the purity of the respective samples. Transcript analysis for the housekeeping gene *pfaldolase* encoding for the enzyme aldolase (Knapp *et al*., 1990) was used as loading control (Fig. 1C). Sample preparations lacking reverse transcriptase were used to investigate possible contamination with genomic DNA and no PCR products were detected (Fig. S1A).

Mouse antisera were generated against two recombinant PPLP2 peptides to investigate protein expression

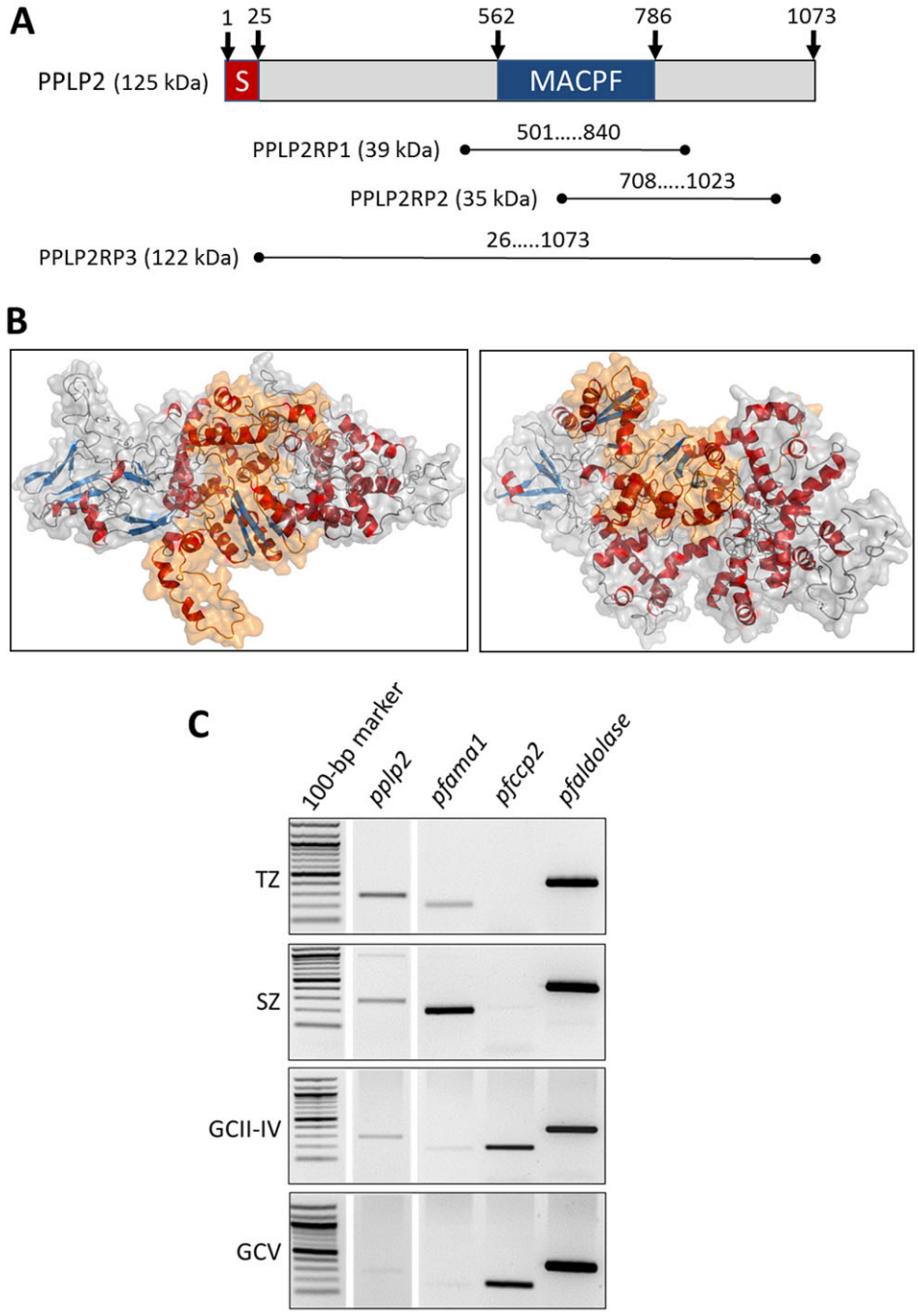

Fig. 1. PPLP2 is expressed in the asexual blood and gametocyte stages of *P. falciparum*.
A. Domain structure of *P. falciparum* PPLP2. The signal peptide (S; red box) and the MACPF domain (blue box) are represented. The underlined regions denote the regions of the recombinant proteins. Arrows indicate amino acid positions.
B. 3D-surface model of PPLP2. The central MACPF domain is highlighted in orange. Alpha-helices (red) and beta-pleated sheets (blue) are indicated. The right image shows a rotated overview which includes the ab-inito predicted parts flanking the centre. Left from central, N-terminus; right from central, C-terminus.
C. Analysis of *pplp2* transcript expression. Transcript of *pplp2* was amplified by diagnostic RT-PCR from cDNA generated from RNA of blood stage trophozoites (TZ) and schizonts (SZ) as well as immature (GCII-IV) and mature (GCV) gametocytes. Transcript analysis of *pfama1* and *pfccp2* were used to demonstrate purity of the blood stage and gametocyte samples respectively. Transcript analysis of *pfaldolase* was used for loading control. Results shown are representative for three independent experiments.

in blood stage parasites. One peptide comprised the MACPF domain of PPLP2 (PPLP2RP1), the other peptide comprised the C-terminal part of the MACPF domain and most of the C-terminus of the protein (PPLP2RP2; see Fig. 1A). Both antisera were able to detect PPLP2 in the blood stages of *P. falciparum* in indirect immunofluorescence assays (IFAs). PPLP2 first appeared in the trophozoites stage and here localized in vesicular structures (Fig. 2A). Multiple PPLP2-positive vesicular structures were detected also in mature schizonts. The blood stage parasites were highlighted by labelling of MSP1 (merozoite surface protein 1; Hall *et al*., 1984). These immunolabelling data are in accordance with findings by Garg *et al.* (2013), who reported PPLP2 expression in the trophozoites and schizonts of *P. falciparum*.

Furthermore, PPLP2 was present in gametocytes, where it was also localized in vesicular structures (Fig. 2B). The gametocytes were highlighted by labelling of Pfs230, a secreted protein abundantly present on the parasite plasma membrane (PPM) of male and female gametocytes (reviewed in Williamson, 2003; Pradel, 2007), and labelling for PPLP2 was found in the majority of the Pfs230-positive gametocytes (89.7 ± 1.6%; mean ± SEM in three independent experiments; $n = 200$). Further, female gametocytes were counter-labelled with antibodies directed against the female-specific protein Pfs25 (reviewed in Pradel, 2007) and PPLP2 was detected in the majority of the Pfs25-positive cells (80.2 ± 2.2%; mean ± SEM in three independent experiments; $n = 200$), in conclusion indicating that PPLP2 is present in gametocytes of both genders. This is in accordance with our previous reports that PPLP2 can be detected both in male and female gametocytes (Deligianni *et al*., 2013). Antisera from non-immunized mice were used for negative control and did not result in any immunolabelling of the gametocytes (Fig. S1B).

Discharge of PPLP2 from gametocytes depends on intracellular calcium

We then investigated the fate of the PPLP2-positive vesicular structures during activation of the gametocytes. Following the first 2 min post activation (p.a.) of the mature gametocytes, the PPLP2-positive structures relocated to the gametocyte periphery (Fig. 2B). At approximately 10 min p.a., when the gametocytes had fully rounded up, the PPLP2 labelling was reduced and a focused dot-like labelling was occasionally visible. Once the gametes had emerged, the PPLP2 labelling had ceased. For example, exflagellating microgametocytes were negative for PPLP2 (Fig. 2B). The data suggest that PPLP2 is located in vesicles, which discharge the perforin between 2–10 min p.a., thus after PVM disintegration but prior to EM rupture (Sologub *et al*., 2011).

We next investigated, if PPLP2 localizes in the gametocytes' osmiophilic bodies. These vesicular electron-dense organelles, which are more abundant in female gametocytes, are crucial for the egress of the activated gametocytes by discharging their content into the parasitophorous vacuole lumen (Sinden *et al*., 1976; Sinden, 1982). We used for these experiments a transgenic *P. falciparum* line, which lacks the osmiophilic body-specific protein Pfg377. The Pfg377-deficient (Pfg377(–)) gametocytes exhibit a reduced number of osmiophilic bodies and are impaired in host cell egress following activation (de Koning-Ward *et al*., 2008). IFAs detected PPLP2 in the Pfg377(–) gametocytes in a labelling pattern comparable to wild-type (WT) gametocytes (Fig. 2C). For control, a female Pfs25-positive WT gametocyte immunolabelled with anti-PPLP2 antisera is shown in Fig. 2C. Furthermore, fluorescence intensity measurements following IFAs demonstrated that PPLP2 and Pfg377 do not colocalize in mature gametocytes (Fig. S1C and D). Noteworthy, Pfg377 labelling is mostly detected in vesicles located at the gametocyte periphery, while in non-activated mature gametocytes PPLP2-positive vesicles are located inwardly. The combined data suggest that PPLP2 is not located in Pfg377-positive osmiophilic bodies.

Garg *et al.* (2013) reported that in schizonts PPLP1 is located in the micronemes and that its discharge depends on intracellular calcium. PPLP1 discharge into the medium can be inhibited by addition of the intracellular calcium chelator BAPTA-AM. In this context, we

Fig. 2. PPLP2 localizes to vesicular structures in the asexual blood and gametocyte stages of *P. falciparum*.
A. PPLP2 localization in asexual blood stage parasites. PPLP2-positive vesicular structures are present in the cytoplasm of trophozoites (TZ) and schizonts (SZ). PPLP2 was immunolabelled with mouse anti-PPLP2RP1 antisera (green), the asexual blood stages were visualized by rabbit anti-MSP1 antisera (red). Nuclei were highlighted by Hoechst stain (blue).
B. PPLP2 localization in gametocytes and relocalization upon activation. PPLP2-positive vesicles (green) are present in mature gametocytes (mGC) and in gametocytes at 2 min p.a. (aGC). Focal PPLP2 labelling is detectable in aGC at 10 min p.a., but not in aGC that have egressed from the RBC. Gametocytes were visualized by rabbit anti-Pfs230 antisera (red); nuclei were highlighted by Hoechst stain (blue). Arrows indicate microgametes.
C. Presence of PPLP2-positive vesicles in Pfg377(–) gametocytes. Immunolabelling as in B; Pfg377(–) gametocytes were visualized by rabbit anti-Pfs230 antisera, female WT gametocytes were visualized by rabbit anti-Pfs25 antisera (red). Images A–C show labelling with antisera directed against PPLP2RP1, a similar labelling pattern was observed for antisera against PPLP2RP2. Results shown in A–C are representative for three to five independent experiments. Bar, 5 μm.

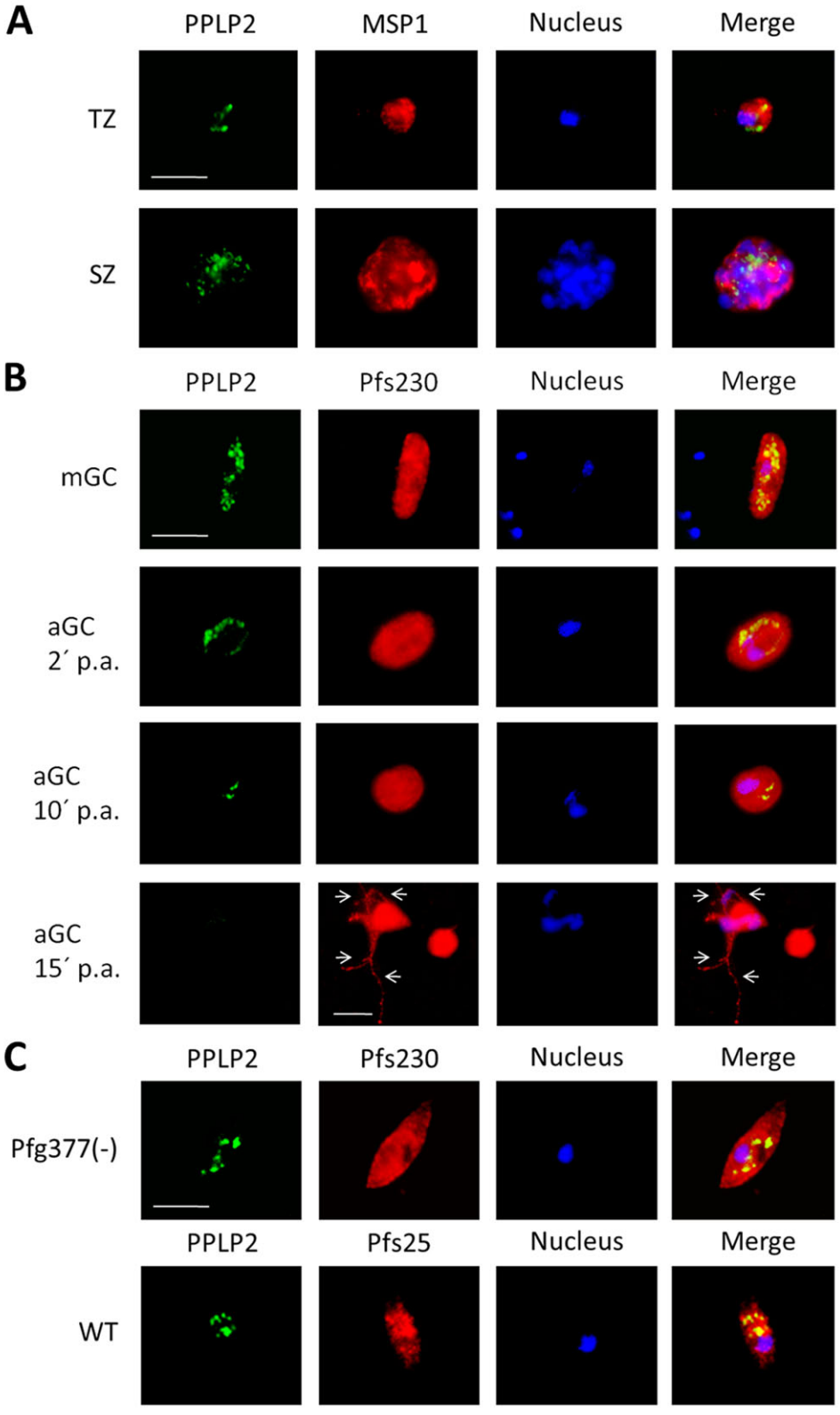

previously demonstrated that BAPTA-AM-treatment of gametocytes during activation results in parasites trapped within the EM, while the PVM has ruptured (Sologub *et al.*, 2011). We thus wanted to investigate, if BAPTA-AM also had an effect on the discharge of the vesicular PPLP2 following gametocyte activation. We treated gametocytes with BAPTA-AM during activation and investigated the localization of the PPLP2-positive vesicular structures between 0–20 min p.a. by IFA. Contrary to untreated activated gametocytes, the PPLP2-positive vesicular structures remained within the activated gametocytes and did not relocate to the gametocyte periphery, when these were treated with BAPTA-AM (Fig. S2). The combined data let us conclude that PPLP2 is located in (Pfg377-negative) vesicles in gametocytes of both genders and that the protein is discharged in a calcium-dependent manner upon gametocyte activation.

The erythrocytic cycle is not affected in PPLP2(–) parasites

For functional characterization of PPLP2, we generated a PPLP2(–) parasite line. The *pplp2* gene locus was disrupted via single cross-over homologous recombination within the MACPF-encoding region, using the pCAM-BSD disruption plasmid (Fig. 3A). Disruption of the *pplp2* gene locus was verified for a clonal line via diagnostic PCR (Fig. 3B). For negative control a parasite line that underwent the transfection procedure in the absence of the pCAM-BSD vector was generated and was subsequently cultured in regular medium (mock control). The absence of PPLP2 in PPLP2(–) gametocytes and blood stage schizonts was demonstrated by IFA (Figs 3C and S3A).

The PPLP2(–) line was first analysed for its potency to replicate in the RBCs. Giemsa smears revealed that the PPLP2(–) blood stages show normal morphologies, when compared with Giemsa smears from WT blood stages (Fig. S3B). To assess the effect of PPLP2 deletion on replication, we subsequently performed a comparative analysis of the PPLP2(–) versus the WT blood stage cycle. Synchronized cultures of WT and PPLP2(–) parasites showed the same percentage of infected erythrocytes at the beginning of the second replication cycle (day 3) in synchronized cultures with the adjusted parasitemia on day 1 (Fig. 4A), suggesting the same efficiency of parasite replication in WT and PPLP2(–) parasites. When the parasitemia was compared between WT and PPLP2(–) blood stage parasites over a period of 7 days (3.5 cycles), parasitemia reached more than 35% for WT and more than 25% for PPLP2(–) parasites (Fig. S3C). However, parasitemia was reproducibly lower in PPLP2(–) cultures than in WT cultures due to increased gametocyte production in the PPLP2(–) cultures (4.87 ± 0.69-fold increase on day 7, mean ± SEM, $n = 3$). This might be explained by the constant exposure of PPLP2(–) parasites to blasticidin, which is known to stimulate gametocyte production (Regev-Rudzki *et al.*, 2013).

Time-lapse recordings of PPLP2(–) parasite invasion revealed a normal pattern of invasion steps, followed by erythrocyte crenation and subsequent relaxation, when the ring form of the parasite became detectable (Fig. 4A, see images). Invaded PPLP2(–) merozoites exhibited active movement inside erythrocytes along with a constant amoeboid shape change (Movie S1), described for *P. falciparum* (Grüring *et al.*, 2011). Next, we assessed the length of the entire erythrocyte cycle (time between cycle initiation and parasite egress) for WT and PPLP2(–) parasites. Synchronized cultures were tested for egress during a time period of 40–52 h post cycle initiation. The result, presented as a cumulative egress kinetics (Fig. 4B), showed no difference between the length of the cycle for WT and PPLP2(–) parasites. Half of WT and PPLP2(–)-infected erythrocytes released parasites between 48 and 49 h post cycle initiation, suggesting that both parasite maturation and merozoite egress were not affected by PPLP2 deletion.

Furthermore, time-lapse recordings of parasite egress showed no differences in this multistep process between WT and PPLP2(–) parasites (Movie S2). Permeabilization of the EM, described earlier for the 3D7 strain of *P. falciparum* (Glushakova *et al.*, 2010) preceded egress of PPLP2(–) parasites, as judged by phalloidin influx using Alexa Fluor 488® phalloidin, a binding partner of erythrocyte cytoskeletal actin, into the erythrocytes. Fig. 4C shows the selected images of a time-lapse recording (Movie S3) of PPLP2(–) parasite egress in the presence of fluorescent phalloidin in the medium. The schizont approaching egress had no detectable fluorescence associated with the EM due to membrane integrity (DIC and fluorescent images on the left), however a few seconds prior to egress the EM became permeable to phalloidin, seen as a bright rim on the periphery of the erythrocyte (images in the centre), followed by rupture of the labelled EM and parasite egress (images on the right). The average time between membrane permeabilization and parasite egress was 13.9 ± 3.7 s (mean ± SEM in 10 independent recordings).

Analysis of PPLP2(–) parasite egress sites by light microscopy revealed full separation of merozoites from each other and from the food vacuole (Fig. 4D). Sites had the expected number of merozoites produced per schizont in each replication cycle. Fig. 4D shows a representative egress site composed of scattered merozoites (white arrow), the food vacuole filled with haemozoin (black arrow), and the remnants of the EM (black arrowhead). This site has at least 25 individual merozoites.

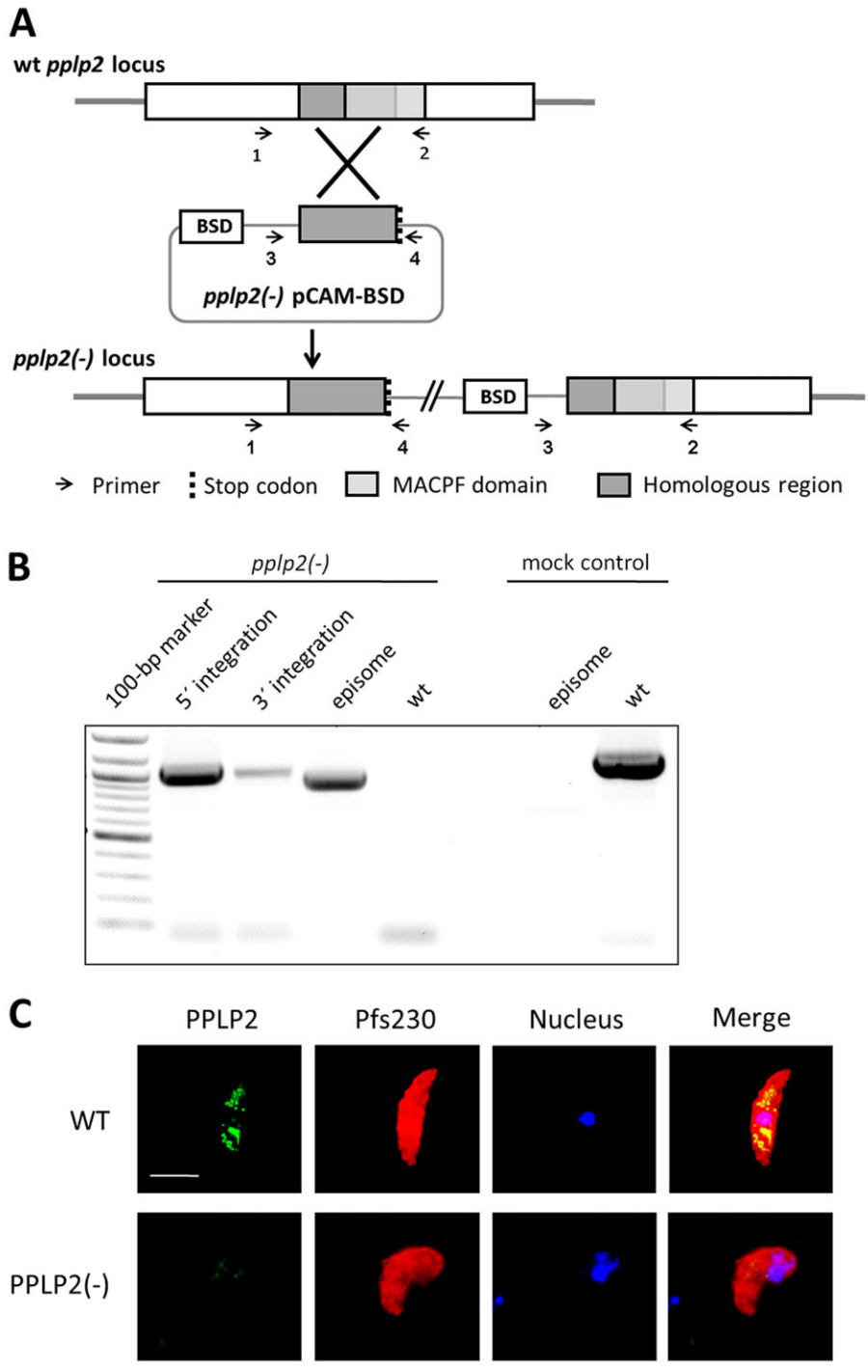

Fig. 3. Generation of a PPLP2(–) parasite line.
A. Schematic diagram of the single-crossover homologous recombination strategy. Arrows with numbers indicate position of primers used to confirm integration of disruption vector *pplp2(–)* pCAM-BSD.
B. Diagnostic PCR demonstrating integration of *pplp2(–)* pCAM-BSD. PCR amplification demonstrates successful 5′-integration (using primers 1 and 4; see A) and 3′-integration (using primers 3 and 2) of pCAM-BSD. Further episomal DNA was amplified (primers 3 and 4), while WT *pplp2* locus DNA is not present (primers 1 and 2). The mock control exhibiting the WT *pplp2* locus is negative for episomal DNA. Results shown are representative for five independent experiments.
C. Absence of PPLP2 in PPLP2(–) gametocytes. Following immunolabelling with mouse anti-PPLP2RP2 antisera, no PPLP2 signal is detected in PPLP2(–) gametocytes via IFA, while in WT gametocytes PPLP2-positive vesicles are present (green). The gametocytes were visualized by rabbit anti-Pfs230 antisera (red), nuclei were highlighted with Hoechst stain (blue). Results shown are representative for two independent experiments. Bar, 5 μm.

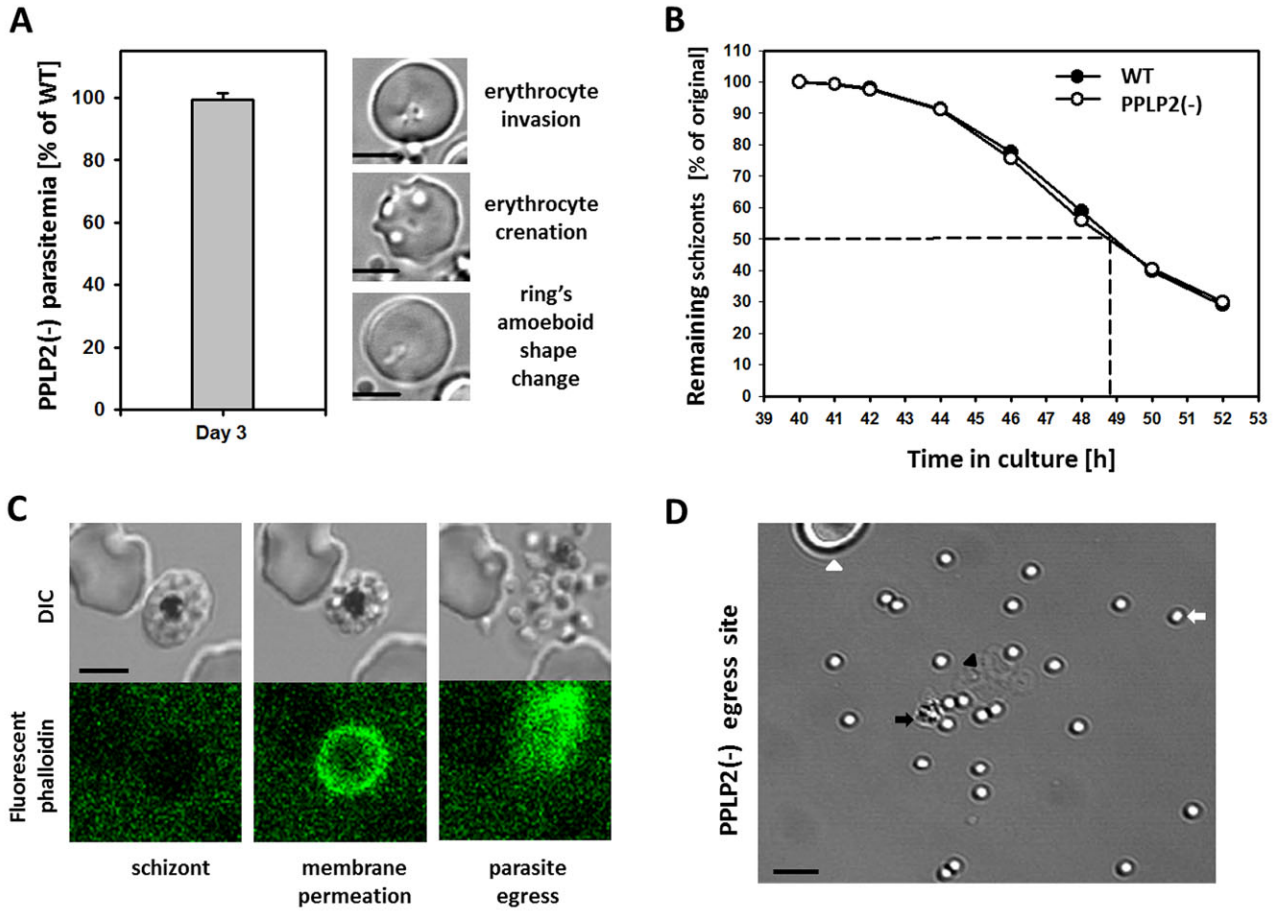

Fig. 4. The erythrocytic cycle of *P. falciparum* is not affected by the absence of PPLP2.
A. Parasite invasion and replication in erythrocytes. The assays show similar invasion and replication behaviour for WT and PPLP2(–) parasites. Images represent the characteristics for *P. falciparum* sequential changes of erythrocyte shape upon PPLP2(–) merozoite invasion: membrane invagination at the place of invasion (upper image), a transient erythrocyte crenation (middle image), and the amoeboid ring within the relaxed erythrocyte (lower image).
B. Cumulative parasite egress kinetics. Egress kinetics show that WT and PPLP2(–) parasites have the same asexual replication cycle length. Dotted lines show that half of WT and PPLP2(–) schizonts finish the cycle between 48 and 49 h post infection initiation.
C. Selected frames from DIC (upper images) and fluorescence (lower images) time-lapse recording of PPLP2(–) merozoites during RBC egress in medium supplemented with fluorescent phalloidin. Permeabilization of the erythrocyte membrane precedes membrane rupture and parasite egress from erythrocytes infected with PPLP2(–) parasites. Selected frames from DIC (upper images) and fluorescence (lower images) time-lapse recording of parasite egress in the medium supplemented with fluorescent phalloidin. Membrane permeabilization leads to Alexa Fluor 488® phalloidin influx into the cell and binding with the erythrocyte cytoskeletal F-actin.
D. Microscopic analysis of merozoite separation. Site of PPLP2(–) parasite egress shows full separation of 26 released merozoites. Black arrow, food vacuole; white arrow, merozoite; black arrowhead, fragments of erythrocyte membrane; white arrowhead, erythrocyte. Results shown in A–D are representative for five independent experiments. Bar, 3 μm (A, C), 15 μm (D).

Thus, PPLP2(–) parasites show normal invasion and egress behaviours.

PPLP2(–) gametocytes are impaired in egress from host erythrocytes

The PPLP2(–) blood stages were able to enter the sexual pathway and formed gametocytes. The morphology of the PPLP2(–) gametocytes during maturation from stage II to stage V was normal, as compared with Giemsa smears of WT gametocytes (Fig. S4A). Upon activation of the mature gametocytes, however, they were unable to exflagellate and misshapen activated microgametocytes were occasionally observed (Fig. S4A). In these cases thick cytoplasmic bundles were protruding from the residual body of the activated microgametocyte, representing the previously described superflagella (Deligianni *et al.*, 2013). The superflagella were also observed in IFA images of activated microgametocytes, which were labelled with antisera against Pfs230 (Fig. S4B).

The efficiency of PPLP2(–) microgametocytes to exflagellate was quantified via exflagellation assays.

Compared with activated WT gametocytes, exflagellation of PPLP2(–) microgametocytes at 15 min p.a. was reduced by 98.9% (Fig. 5A). This led to a significantly decreased transmission of PPLP2(–) parasites to mosquitoes, as was demonstrated in standard membrane feeding assays (SMFAs). PPLP2(–) gametocytes were fed to *Anopheles stephensi* mosquitoes in five independent experiments. The numbers of oocysts were counted at 10–12 days post feeding and compared with the oocyst numbers of feeds with WT gametocytes and with mock control gametocytes. The SMFAs showed a significant reduction in the numbers of oocysts per infected mosquito, when compared with the controls (Fig. 5B; Table 1).

We then investigated the ultrastructure of the PPLP2(–) gametocytes before and after activation. Gametocytes were activated *in vitro* and samples were fixed at 0, 7 and 15 min p.a. Non-activated WT gametocytes were enveloped by three membranes, the EM, the PVM and the PPM. Right underneath the PPM the thick double membrane of the inner membrane complex (IMC) was observed. At 7 min p.a., the PVM of WT gametocytes had disappeared, while EM breakdown occurred at approximately 15 min p.a. (Fig. 6A, left panels). This observation is in accordance with our previous reports on the inside-out egress of activated gametocytes (Sologub *et al.*, 2011; reviewed in Wirth and Pradel, 2012). Mature PPLP2(–) gametocytes exhibited an ultrastructure comparable to WT, including the IMC and the two enveloping membranes (Fig. 6A, right panels). Noteworthy, osmiophilic bodies were observed in the ultrasections of PPLP2(–) gametocytes, indicating that the loss of PPLP2 does not affect these organelles. At 7 min p.a., the PVM of the PPLP2(–) gametocytes had ruptured normally, and fragments of the PVM as well as PVM-derived membrane layers (PDMs) were regularly observed. However, contrary to the WT, the erythrocyte cytoplasm (EC) was still visible. At 15 min p.a., thus at a time point when the WT gametocytes had egressed from the remnants of the EM, the PPLP2(–) gametocytes were still trapped within the intact RBC (Fig. 6A, right panel). Similar to WT gametocytes, axonemes were regularly detected and the IMC was partially disintegrated in the PPLP2(–) gametocytes. Trapping of activated PPLP2(–) gametocytes inside the enveloping RBC was observed for both males (Fig. 6A) and females (Fig. 6B).

At 15 min p.a., 84% of the activated PPLP2(–) gametocytes were unable to egress from the enveloping erythrocyte, and 28% of these parasites had axonemes ($n = 50$; three independent experiments were used for quantification). Only 16% of the PPLP2(–) parasites had developed into male and female gametes with a normal ultrastructure (a female fertile gamete is shown in Fig. S4C).

In some cases, superflagella were observed, which protruded from one site of the activated PPLP2(–) microgametocytes (Figs 6C and S4D). The superflagella were enveloped by both PPM and EM, and EC was observed between these two membranes. The PPLP2(–) superflagella are similar to axoneme bundles previously observed in gametocytes treated before activation with the protease inhibitor 1,10-phenanthroline (Sologub *et al.*, 2011). These axoneme bundles were also covered by PPM and EM, as shown by transmission electron microscopy on protease inhibitor-treated activated microgametocytes (Fig. S5A). Contrary to activated PPLP2(–) microgametocytes, no EC was observed in the host RBCs, indicating that 1,10-phenanthroline treatment does not affected EC release.

The combined data show that activated PPLP2(–) gametocytes were unable to release the EC and to rupture the EM. Other morphological changes, like axoneme formation and IMC disintegration were not impaired. Thus, fully developed PPLP2(–) gametes of both genders were apparently trapped within the host erythrocyte. We conclude that PPLP2 might play a role in EM permeabilization, which is preparing the enveloping EM for rupture.

Permeabilization of the erythrocyte membrane is essential for gametocyte egress

To directly demonstrate the putative EM permeabilization prior to gametocyte egress, we subjected activated gametocytes to live cell microscopy in the presence of fluorescent Alexa Fluor 488® phalloidin. As described above for merozoite egress, phalloidin labels the erythrocyte cytoskeleton upon influx inside the cells through the perforated membranes. We showed that EM permeabilization occurred prior to membrane rupture and membrane shedding from activated gametocytes (Fig. 7A). Average time intervals were equal to 6.27 ± 0.93 min between gametocyte activation and subsequent EM permeabilization and to 9.03 ± 1.54 min between gametocyte activation and egress (Fig. 7B, $n = 10$). The mean calculated time between EM permeabilization and gametocyte egress was 2.76 ± 0.80 min, which is approximately 15 times longer than the same parameter for merozoite egress from erythrocytes. This observation suggests that the mechanisms of parasite egress from infected erythrocytes at the end of the asexual replication cycle and those occurring upon gametocyte activation may be different. EM permeabilization was observed in rounded activated gametocytes and coincided with a significant drop in the optical density of EC compartment (Movie S4), suggesting a causative relationship between EM permeabilization and haemoglobin diffusion from erythrocytes. Live cell microscopy of PPLP2(–) activated gametocytes, on the other hand, did not reveal the same sequence of events that was

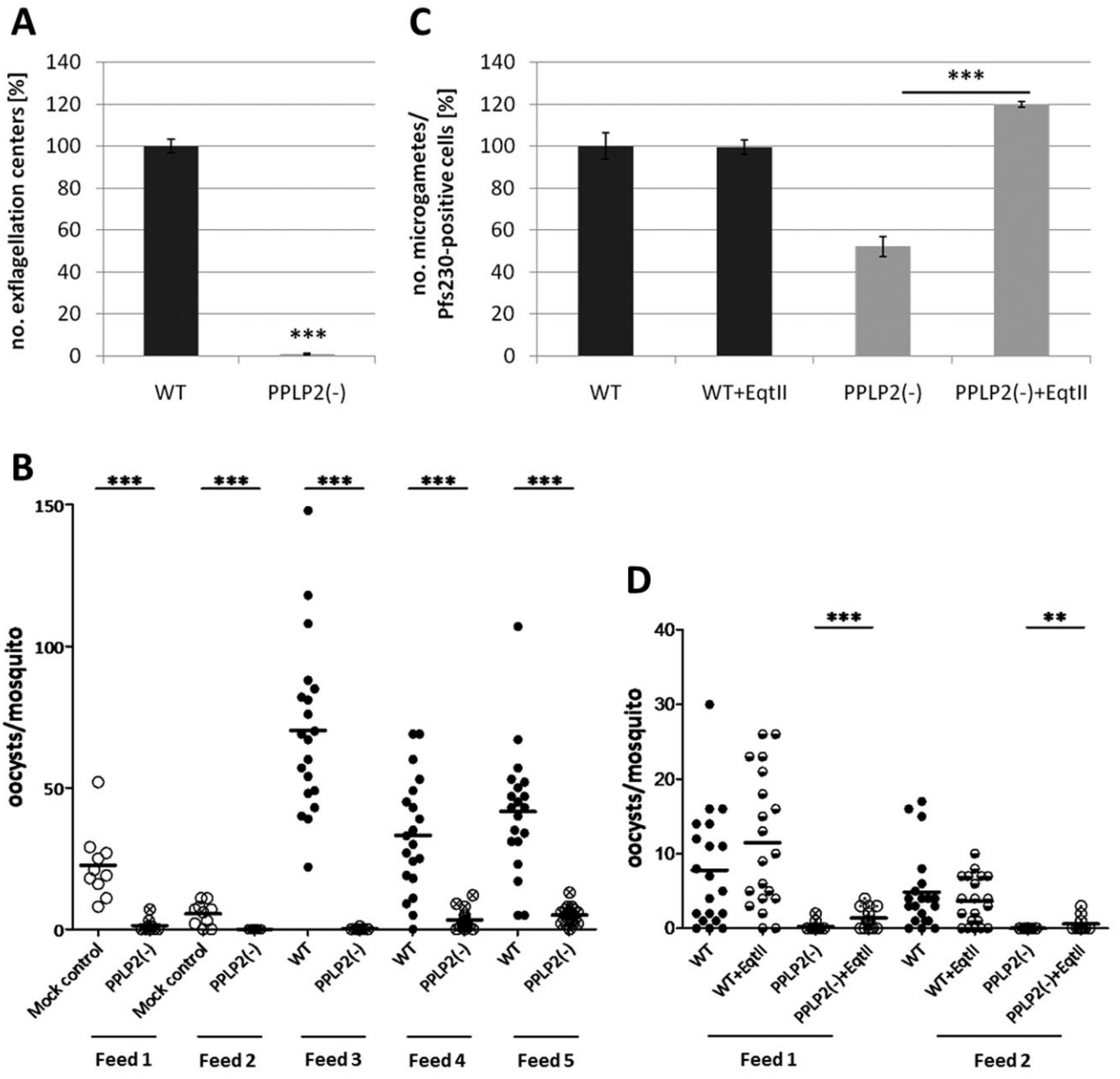

Fig. 5. PPLP2(–) parasites are impaired in transmission to mosquitoes, but rescued by equinatoxin II treatment.
A. PPLP2(–) gametocytes are blocked in exflagellation. The number of exflagellation centres at 15 min p.a. of mature gametocytes is significantly reduced in the PPLP2(–) cultures compared with WT (set to 100%). Experiments were done in triplicate (mean ± SEM). ***$P \leq 0.001$ (Student's *t*-test).
B. PPLP2(–) gametocytes show reduced transmission to mosquitoes. The numbers of oocysts per midgut are significantly lower following infection of *An. stephensi* mosquitoes with PPLP2(–) gametocytes in SMFAs than following feeds with WT and mock control. ***$P \leq 0.001$ (Student's *t*-test).
C. Rescue of PPLP2(–) exflagellation by equinatoxin II. The numbers of exflagellation centres at 15 min p.a. of mature gametocytes is significantly increased in equinatoxin II-treated PPLP2(–) compared with DMSO-treated PPLP2(–), while no difference is observed in exflagellation of equinatoxin II-treated and DMSO-treated WT (set to 100%). Experiments were done in triplicate (mean ± SEM). ***$P \leq 0.001$ (Student's *t*-test).
D. Increased transmission of PPLP2(–) gametocytes to mosquitoes following equinatoxin II treatment. The numbers of oocysts per midgut are significantly higher in *An. stephensi* mosquitoes infected with PPLP2(–) gametocytes treated with equinatoxin II compared with untreated PPLP2(–). **$P \leq 0.01$; ***$P \leq 0.001$ (Student's *t*-test).

Table 1. Standard membrane feeding assays with PPLP2(–).

	Feed	Infections/total (*n*)	Oocysts/midguts (mean ± SD, range)	Infection rate (%)	Change in transmission (%)
Experimental setting 1: PPLP2(–) versus WT					
Feed 1	Mock control	10/10	23 ± 12, 8–52	100	/
	PPLP2(–)	5/10	1 ± 2, 0–7	50	–50
Feed 2	Mock control	8/10	6 ± 4, 0–11	80	/
	PPLP2(–)	0/10	0 ± 0, 0	0	–100
Feed 3	WT	20/20	70 ± 30, 22–148	100	/
	PPLP2(–)	4/20	0 ± 0, 0–1	20	–80
Feed 4	WT	19/20	33 ± 20, 0–69	95	/
	PPLP2(–)	17/20	3 ± 3, 0–12	85	–11
Feed 5	WT	20/20	42 ± 22, 5–107	100	/
	PPLP2(–)	19/20	5 ± 3, 0–13	95	–5
Experimental setting 2: Equinatoxin II (EqII) treatment					
Feed 1	WT	17/20	8 ± 8, 0–30	85	/
	WT + EqtII	18/20	11 ± 9, 0–26	90	+6
	PPLP2(–)	4/20	0 ± 1, 0–2	20	/
	PPLP2(–) + EqtII	14/20	1 ± 1, 0–4	70	+250
Feed 2	WT	17/20	5 ± 5, 0–17	85	/
	WT + EqtII	15/20	4 ± 3, 0–10	75	–12
	PPLP2(–)	1/20	0 ± 0, 0–1	5	/
	PPLP2(–) + EqtII	5/20	0 ± 1, 0–2	25	+400

observed for WT gametocytes (Fig. 7C). Rounded activated gametocytes were found in phalloidin-impermeable erythrocytes in 90% of observed cells ($n = 31$). The EM often was blebbed, which suggests normal erythrocyte cytoskeletal digestion by gametocytes before their departure from the host cells. Thus, the revealed sequence of events observed upon activation of WT gametocytes, i.e. rounding of infected cells, EM permeabilization and membrane shedding, was blocked in the PPLP2(–) gametocytes.

Subsequently, we evaluated if EM permeabilization is a prerequisite for gametocyte egress from the erythrocyte. We thus studied the effect of the pore-forming toxin equinatoxin II on promoting exflagellation of activated PPLP2(–) gametocytes. Equinatoxin II was previously shown to selectively permeabilize the EM of *P. falciparum*-infected erythrocytes without affecting the integrity of the PVM (Jackson *et al*., 2007). Equinatoxin II was successfully used to rescue *P. berghei* PPLP2(–) gametocytes trapped within the erythrocyte (Deligianni *et al*., 2013). To confirm the effect of equinatoxin II on erythrocytes, we incubated these with the toxin, which resulted in erythrocyte lysis and haemoglobin release into the medium (data not shown). We then treated activated PPLP2(–) gametocytes with equinatoxin II prior to activation and quantified the numbers of microgametes at 15 min p.a. via IFA. Microgamete numbers significantly increased in the equinatoxin II-treated gametocyte cultures compared with untreated PPLP2(–) control (Fig. 5C). As expected, the numbers of oocysts attached to the midguts of mosquitoes infected with equinatoxin II-treated PPLP2(–) parasites also increased in the SMFAs, when compared with feeds with untreated PPLP2(–) cultures (Fig. 5D; Table 1). The experiments demonstrate that the PPLP2(–) loss-of-function phenotype can be reversed by artificial permeabilization of the EM.

As described above, in activated WT gametocytes, the EC disappears within less than 5 min after PVM rupture, but more than 5 min before rupture of the EM. In the PPLP2(–) gametocytes, on the other hand, the EC does not disappear following PVM rupture. Because discharge of the PPLP2-positive vesicles can be inhibited by BAPTA-AM treatment, we wanted to know, if in BAPTA-AM-treated activated gametocytes the EC was present. Transmission electron microscopy on the chelator-treated gametocytes showed that in 75% of gametocytes the EC was present ($n = 20$; Fig. S5B). We had previously described that treatment of gametocytes with TLCK before activation inhibits the EM rupture, while E64d impairs PVM breakdown (Sologub *et al*., 2011). When we re-investigated the ultrastructure of activated gametocytes treated with the two protease inhibitors ($n = 20$ per inhibitor), we observed that in all cases the EC was missing (Fig. S5C and D). These data show that BAPTA-AM but not the protease inhibitors interfere with EC release and indicate that PVM disintegration, EC release, and EM rupture are independent events.

We also investigated the fate of the EC in activated PPLP2(–) versus WT gametocytes in more detail. For both parasite lines, similar numbers of gametocytes per volume were activated and the supernatant was collected at 45 min p.a. Subsequently, the OD_{405} values of the supernatants of activated PPLP2(–) and WT gametocytes were determined to measure the haemoglobin

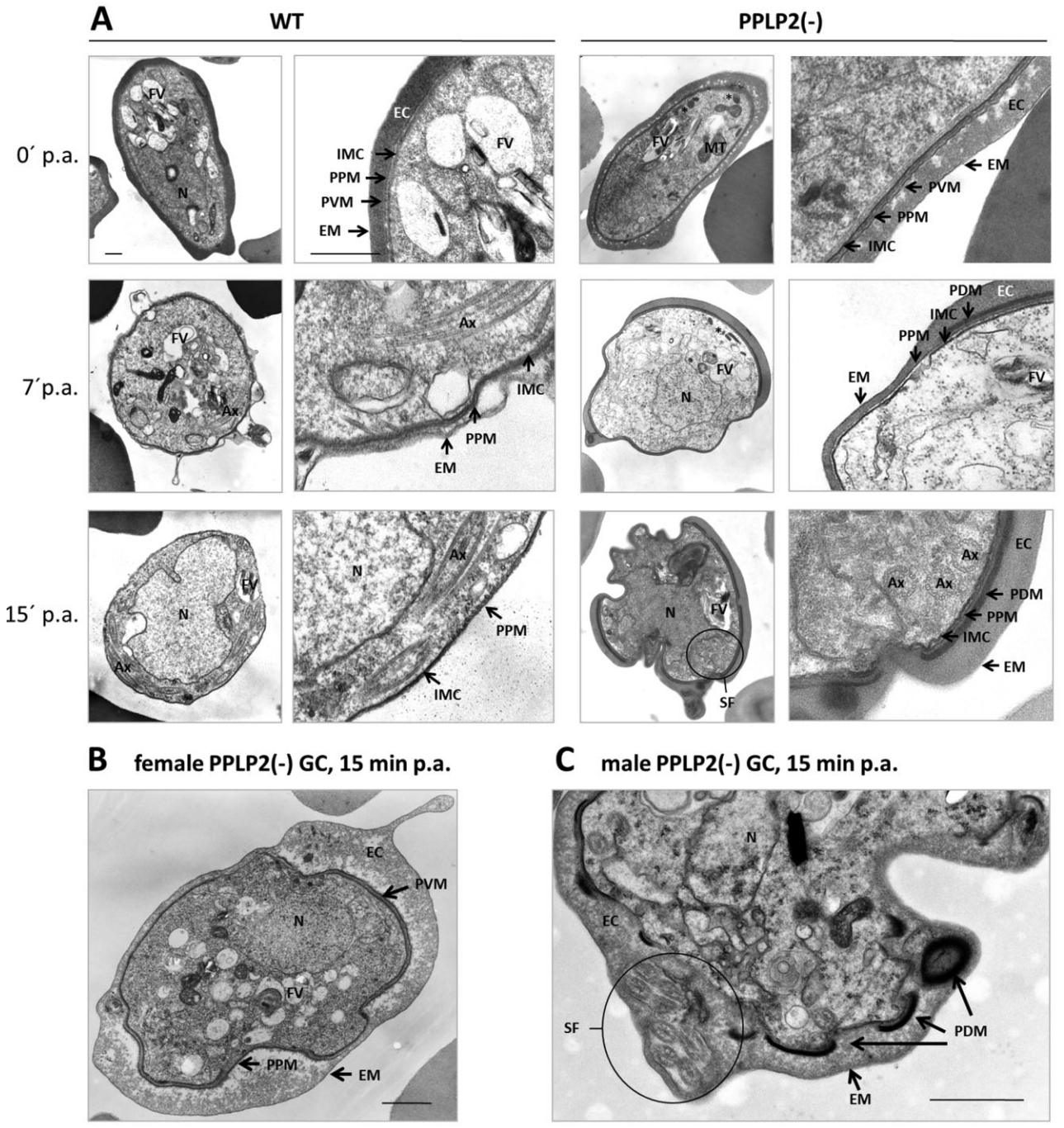

Fig. 6. Activated PPLP2(–) gametocytes are trapped within the erythrocyte.
A. Ultrastructural changes in PPLP2(–) gametocytes following activation compared with WT. Transmission electron microscopic analyses on mature PPLP2(–) gametocytes at 0 min (0′), 7 min (7′) and 15 min (15′) p.a. demonstrates that at 7′ p.a. the PVM is ruptured, but contrary to WT, the EC is still present. At 15′ p.a. the EM remains intact. Asterisks indicate osmiophilic bodies, arrowheads indicate axoneme bundles. Axonemes (Ax) are indicative of male gametocytes.
B. Ultrastructure of an activated female PPLP2(–) gametocyte. At 15 min p.a. the activated female PPLP2(–) gametocyte (GC) is trapped within the erythrocyte.
C. Ultrastructure of the superflagellum. A bundle of eight axonemes is shown in an ultrasection of a PPLP2(–) gametocyte (GC) at 15 min p.a. Results shown in A–C are representative for three independent experiments. Ax, axoneme; EC, erythrocyte cytoplasm; EM, erythrocyte membrane; FV, food vacuole; IMC, inner membrane complex; MT, mitochondrion; N, nucleus; PDM, PVM-derived membrane layers; PPM, parasite plasma membrane; PVM, parasitophorous vacuole membrane; SF, superflagellum. Bar, 500 nm (A), 1 μm (B, C).

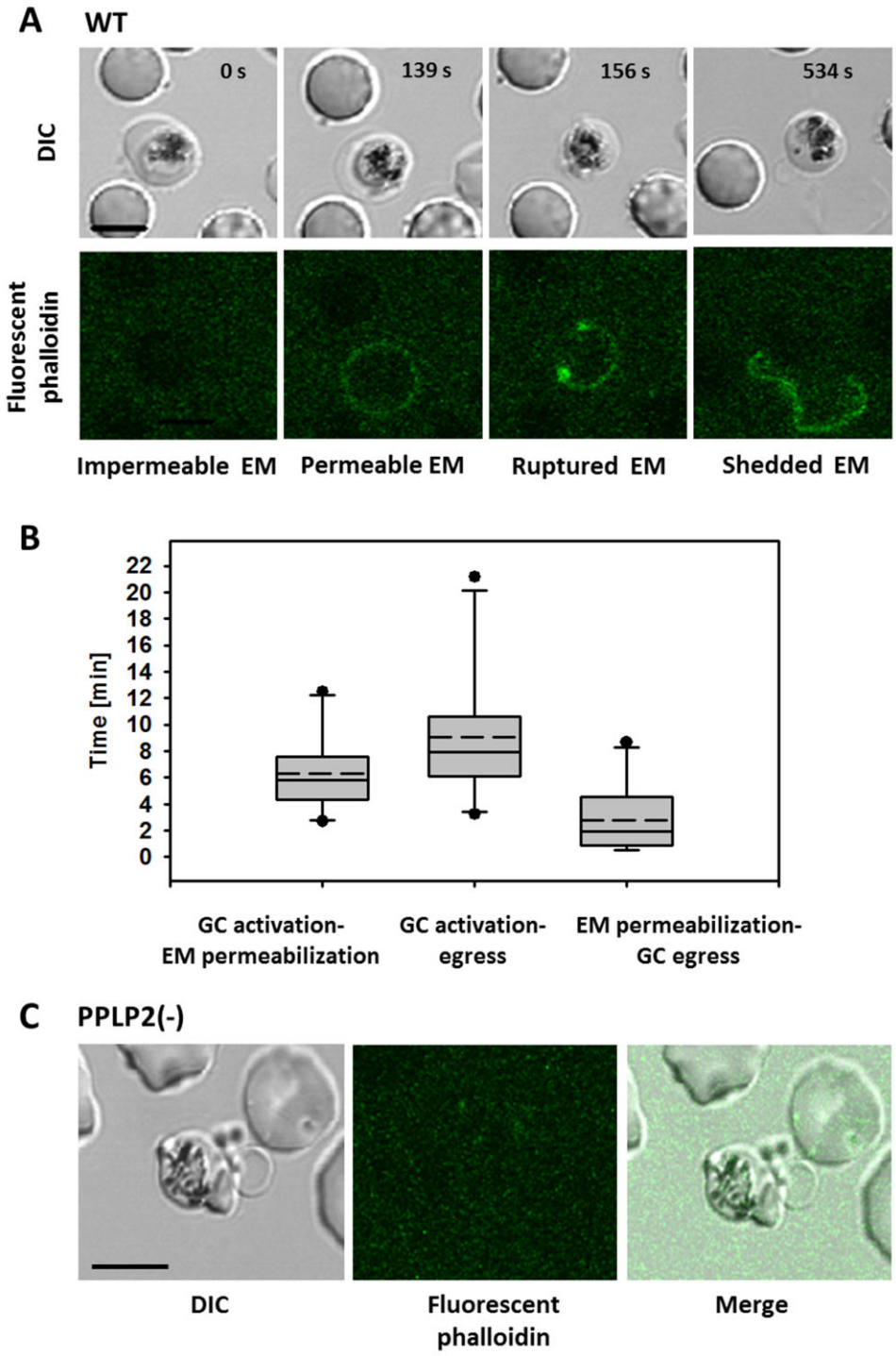

Fig. 7. Erythrocyte membrane permeabilization, rupture and shedding are sequential steps in the egress of activated WT gametocytes which are not observed in activated PPLP2(–) gametocytes.
A. Selected frames from DIC (upper images) and fluorescence (lower images) time-lapse recording of WT activated gametocytes during erythrocyte egress in medium supplemented with fluorescent phalloidin. Alexa Fluor 488® phalloidin was added to WT gametocyte cultures followed by activation. Phalloidin influx into the erythrocytes occurs prior to membrane rupture and membrane shedding from the gametocyte.
B. Time intervals between gametocyte activation, EM permeabilization and gametocyte egress assessed by phalloidin influx. Results are presented as a box plot with median values (solid lines), mean values (dotted lines) and percentiles, $n = 10$. EM, erythrocyte membrane; GC, gametocyte.
C. Activated PPLP2(–) gametocytes do not demonstrate EM permeabilization, membrane rupture and membrane shedding. Phalloidin influx does not occur in activated PPLP2(–) gametocytes. A representative live cell image was taken 30 min p.a.

concentration. The values were normalized per OD_{405} value of supernatant in WT gametocyte culture completely lysed by saponin treatment. The results showed that there was significantly less haemoglobin present in cultures of activated PPLP2(–) gametocytes as compared with WT gametocyte cultures (Fig. 8A), suggesting that in WT gametocytes the EC is released into the medium.

Our data suggested that PPLP2 functions by forming pores in the EM, resulting in the depletion of EC. To test whether PPLP2 possesses EM-lytic activities, we performed an erythrocyte lysis assay, using recombinant full length PPLP2 (PPLP2RP3, see Fig. 1A). His-tagged PPLP2RP3 was expressed in the mammalian expression system and purified by Ni-NTA chromatography (Fig. S6A). Lysis activity of PPLP2RP3 was tested on human erythrocytes. The assay revealed a dose-dependent release of haemoglobin from RBCs above a PPLP2RP3 concentration of 10 nM indicating lysis of erythrocytes by the perforin (Fig. 8B). The addition of PPLP2RP2, on the other hand, had no effect on RBC integrity (data not shown). This might be explained by lack of the intact MACPF domain in PPLP2RP2. Noteworthy, the MACPF domain is crucial for pore formation, while the C-terminal part of perforins is important for the initial interaction with the target membrane and also confers calcium dependence (Voskoboinik *et al.*, 2005; 2006).

To determine, if EM permeabilization is required for gametocyte egress we treated gametocytes with the pore sealant Tetronic 90R4 prior to their activation. The pore sealant prevented exflagellation in a dose-dependent manner, as determined by exflagellation assays (Fig. 8C). For control, we investigated the effect of Tetronic 90R4 on the egress of merozoites and demonstrated a dose-dependent inhibition of WT and PPLP2(–) merozoite egress by this compound (Fig. S6B).

The morphology of the Tetronic 90R4-treated gametocytes was investigated by transmission electron microscopy. While non-activated gametocytes treated with the pore-sealant showed a normal morphology (data not shown), gametocytes at 15 min p.a. were trapped within the host erythrocyte (Fig. 8C). The Tetronic 90R4-treated gametocytes were in the process of rounding up, but the EM remained intact and EC was present. In approximately 50% of the Tetronic 90R4-treated gametocytes, the PVM was also intact ($n = 10$), indicating that the pore sealant might also affect PVM disintegration (Fig. 8D).

Lastly, we investigated the exflagellation activity of PPLP2(–) gametocytes over time. First, we quantified trapped but motile microgametes of a PPLP2(–) culture at 7 different time points between 0–150 min p.a. The assays revealed that the activity of the microgametes peaked at 30 min (Fig. S6C), which coincides with the peak in exflagellation of activated WT gametocyte cultures (e.g. Delves *et al.*, 2013). The PPLP2(–) microgametes kept being motile for another hour before the activity ceased. We then compared the numbers of exflagellation centres (thus of microgametocytes not trapped within the erythrocyte) of the same PPLP2(–) gametocyte culture between day 12, thus when the first mature gametocytes have formed, and day 23. At the later time point, when erythrocytes became prone to lytic deterioration, we observed more exflagellation centres than on day 12 (Fig. S6D). We concluded that PPLP2(–) gametes trapped within the erythrocytes are fully functional and that the gametes' ability to exit the enveloping host cell directly correlates with the aging of the host cell membrane.

Discussion

The egress of *P. falciparum* from the enveloping RBC is a tightly regulated event and involves the sequential rupture of two membranes, the PVM and the EM. The escape from the RBC is crucial for malaria parasite progression through its life cycle that includes replication of asexual blood stages and mating of the newly formed gametes. Several recent publications provided increasing evidence for an inside-out egress of the malaria parasite from the erythrocyte, during which the breakdown of the PVM precedes rupture of the EM (Glushakova *et al.*, 2010; Chandramohanadas *et al.*, 2011; Graewe *et al.*, 2011; Sologub *et al.*, 2011; reviewed in Wirth and Pradel, 2012). However, the molecular mechanisms of the inside-out egress are not fully known yet.

We here show that the *P. falciparum* perforin PPLP2 is crucial for RBC egress by activated gametocytes, but not by merozoites during blood stage schizogony. Initially we investigated the 3D-structure of PPLP2 to receive first clues on a potential pore-forming function of the protein. PPLP2 comprises a MACPF domain, typical for pore-forming proteins, like PF1 (reviewed in Rosado *et al.*, 2008; Dunstone and Tweten, 2012). PF1 is a thin 'key-shaped' molecule, comprising an N-terminal MACPF domain followed by an epidermal growth factor (EGF) domain that, together with the C-terminal sequence, forms a central shelf-like structure. In PF1, a C-terminal C2 domain mediates initial, calcium-dependent membrane binding (Law *et al.*, 2010). Contrary to PF1, the MACPF domain of PPLP2 is located in the centre and PPLP2 has an N-terminal sequence extension not seen in PF1. The C-terminal domain predicted and *ab initio* modelled is clearly different from PF1, e.g. there is no C2 domain present, however, the globular, helical bundle-like structure from the prediction fits well with the functional evidence for calcium-dependent membrane binding.

We showed that PPLP2 is expressed in the asexual blood stages and in gametocytes of both genders. It

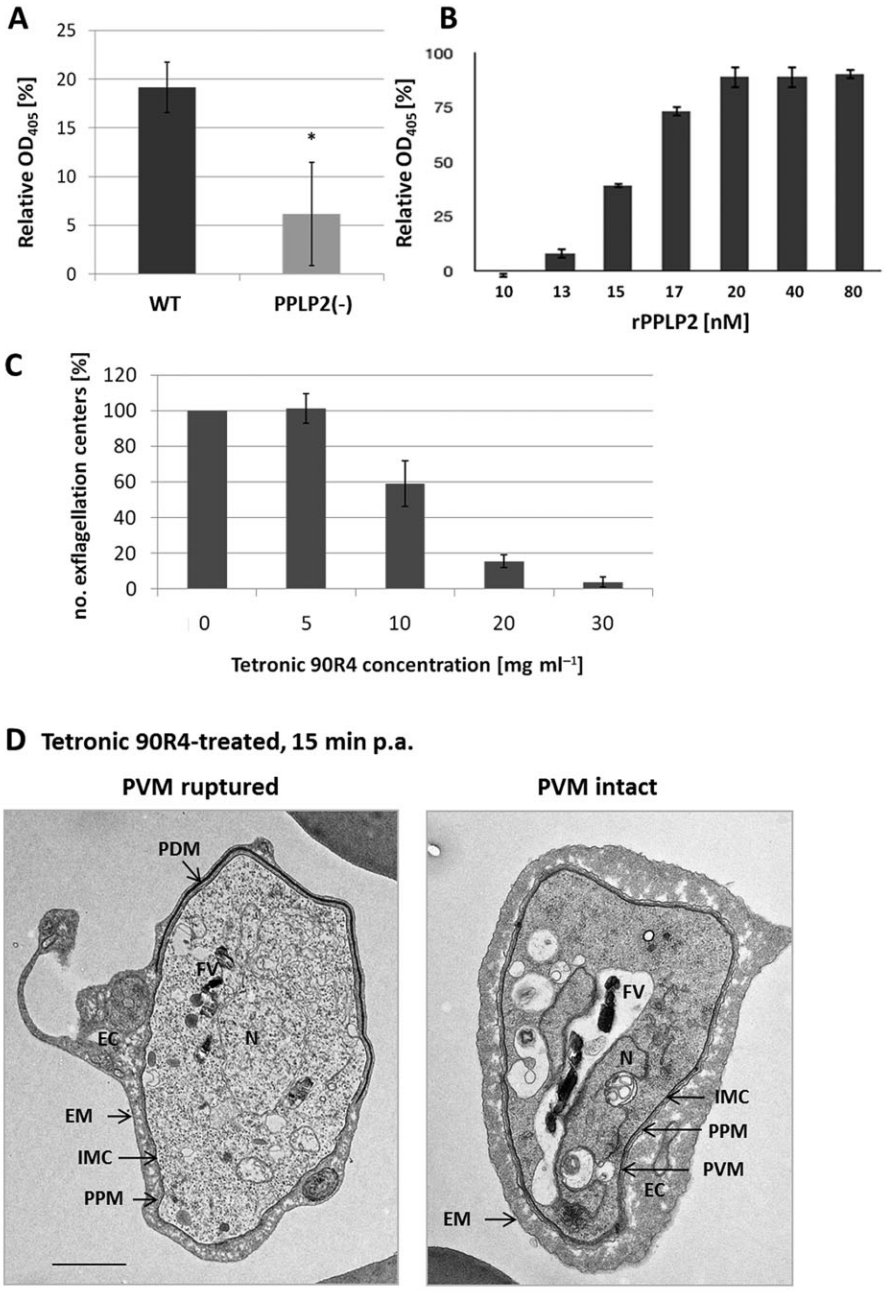

Fig. 8. EM permeabilization is linked to gametocyte egress.
A. PPLP2(–) gametocytes release less haemoglobin upon activation. Haemoglobin in the supernatant of PPLP2(–) versus WT cultures was measured at OD_{405} at 45 min p.a. and expressed as percentage of maximum haemoglobin release in saponin-lysed gametocyte cultures (set to 100%). Experiments were done in triplicate (mean ± SEM). *$P \leq 0.1$ (Student's *t*-test).
B. Lysis of erythrocytes by recombinant PPLP2. Addition of recombinant full length PPLP2 (rPPLP2 = PPLP2RP3) results in the release of haemoglobin from human erythrocytes above a concentration of 10 nM indicating lysis of erythrocytes. Haemoglobin release was measured at OD_{405} and expressed as a percentage of maximum haemoglobin release in erythrocytes lysed in water (set to 100%). Experiments were done in triplicate (mean ± SEM).
C. Inhibition of exflagellation of WT gametocytes by pore-sealant. A dose-dependent reduction in the numbers of exflagellation centres at 15 min p.a. occurs, when gametocyte cultures were treated with Tetronic 90R4 in concentrations between 5 and 30 mg ml^{-1} prior to activation as compared with non-treated cultures (set to 100%). Experiments were done in triplicate (mean ± SEM).
D. Ultrastructure of activated WT gametocytes treated with pore-sealant. At 15 min p.a. the gametocytes remain trapped within the erythrocyte when these were treated with 30 mg ml^{-1} Tetronic 90R4 prior to activation. The EC is present and the PVM is either ruptured (left image) or intact (right image). Results shown are representative for two independent experiments. EC, erythrocyte cytoplasm; EM, erythrocyte membrane; FV, food vacuole; IMC, inner membrane complex; N, nucleus; PDM, PVM-derived membrane layers; PPM, parasite plasma membrane; PVM, parasitophorous vacuole membrane. Bar, 1 μm.

localizes in vesicular structures both in the asexual and sexual forms of the parasite. While the vesicles relocate to the gametocyte surface at approximately 5 min p.a., when the parasite starts to round up, such relocation cannot be seen in the mature schizonts prior to rupture. These observations are in accordance with findings by Garg *et al.* (2013), who reported the relocation of *P. falciparum* PPLP1 but not PPLP2 to the enveloping membranes of the mature schizonts upon discharge from the micronemes.

The egress of the intraerythrocytic merozoites from the RBC can be divided into two stages: pre-egress shape transformation that lasts on average 7 min (Glushakova *et al.*, 2013) and a very rapid egress itself that takes only several seconds. It is the most dramatic membrane rearrangement in the erythrocyte asexual cycle of *P. falciparum* replication that includes EM fragmentation and subsequent vesiculation upon merozoite scattering release from infected RBC at the end of the cycle (Glushakova *et al.*, 2005). The mechanism of this process is not entirely understood, but it includes progressive digestion of the erythrocyte cytoskeleton (Chandramohanadas *et al.*, 2009; Glushakova *et al.*, 2009) and EM permeabilization before membrane rupture (Glushakova *et al.*, 2010; Garg *et al.*, 2013). We examined a potential role of PPLP2 in this process, as well as its putative role in the varieties of membrane reorganizations that happen inside the infected erythrocytes during asexual replication. However, side by side comparison of the asexual erythrocyte cycles in the same sample of blood for WT and PPLP2(–) parasites did not reveal any abnormalities in life cycle progression for PPLP2(–). We observed normal PPLP2(–) merozoite invasion into erythrocytes and the subsequent free movement of the amoeboid rings inside the host cell. This suggests a successful separation of the parasitophorous vacuole from the EM. Parasite maturation and schizogony were successful in PPLP2(–) as well. The length of the erythrocyte asexual cycle and the egress process were the same in WT and PPLP2(–) parasites. EM permeabilization occurred before EM rupture for PPLP2(–) parasites, with kinetics similar to the ones described for *P. falciparum* 3D7 (Glushakova *et al.*, 2010). Sites of parasite egress revealed fully separated PPLP2(–) merozoites and the presence of typical EM fragments close to the egress sites. Thus, PPLP2 is not involved in the events of membrane modification during the parasitic asexual cycle of replication needed for merozoite formation and egress. We conclude that PPLP2 is dispensable for parasite intraerythrocytic asexual development *in vitro*.

Contrary to the rapid release of the intraerythrocytic merozoites from the enveloping RBC, gametocyte egress is a slow process. Although the PVM ruptures rapidly, within approximately 1 min p.a., the parasites remain covered by the EM for another 10 min and only exit the RBC after the gametes have fully developed (Sologub *et al.*, 2011). This delayed egress might provide the developing gamete with enough time to adapt to the mosquito midgut. Notably, we recently showed that following gametocyte activation the plasmodial transmembrane protein PfGAP50 relocates from the IMC to the PPM (Simon *et al.*, 2013). Only after PfGAP50 is relocated to the PPM, the gametes exit the RBC. PfGAP50 enables the newly formed gametes to bind the complement regulatory factor H from the blood meal, thereby evading lysis by human complement factors that had entered the mosquito midgut with the blood meal. Apparently, protection by the EM provides the activated gametocytes with sufficient time to transform into fertile gametes that are able to defend themselves against blood meal factors.

In accordance with the delay in the rupture of the EM we see a relocation of the PPLP2-positive vesicles to the gametocyte periphery at approximately 5 min p.a., when PVM breakdown had already occurred. In line with these observations, gametocytes lacking PPLP2 were able to rupture the PVM, but not the EM, indicating that PVM disintegration does not involve PPLP2 activity. Similar results were obtained by Deligianni *et al.* (2013), who reported that *P. berghei* gametocytes lacking PPLP2 were unable to permeabilize the EM during egress, while PVM rupture was not affected. Contrary to *P. falciparum*, though, in *P. berghei* PPLP2 is only important for the egress of male gametocytes, indicating a gender-specificity of the perforin (Deligianni *et al.*, 2013). PPLP2(–) gametes of *P. berghei* and *P. falciparum* developed normally and were able to fertilize, once the EM had been artificially lysed. In a few cases, malformed activated microgametocytes were observed both in *P. berghei* and in *P. falciparum*, in which the axonemes had assembled to superflagella, probably because the exit of the axonemes from the cytoplasm of the residual gametocytes was not correctly co-ordinated (Deligianni *et al.*, 2013).

PVM rupture is linked to the presence of osmiophilic bodies, which migrate to the PPM during gametocyte activation and then discharge their content into the lumen of the parasitophorous vacuole. An accumulation of osmiophilic bodies can be observed underneath the rupture sites. The vesicles disappear at two minutes p.a., coevally with the disintegration of the PVM (Sologub *et al.*, 2011). Osmiophilic bodies contain a gametocyte-specific protein, Pfg377 (Alano *et al.*, 1995; Severini *et al.*, 1999). *P. falciparum* gametocytes lacking this protein reveal a reduced number of osmiophilic bodies and macrogametocytes fail to egress from the host erythrocyte (de Koning-Ward *et al.*, 2008). Two other proteins are associated with the gametocyte osmiophilic bodies, i.e.

MDV-1/Peg3 (Furuya *et al*., 2005; Silvestrini *et al*., 2005; Lanfrancotti *et al*., 2007; Ponzi *et al*., 2009) and GEST (Talman *et al*., 2011); and PVM rupture was impaired in *P. berghei* gametocytes lacking MDV-1/Peg3 or GEST (Ponzi *et al*., 2009; Talman *et al*., 2011). The combined data suggest that the discharge of the osmiophilic body content is particularly important for PVM rupture. Noteworthy, PPLP2 is expressed in Pfg377(–) gametocytes, indicating that the protein is not located in the (Pfg377-positive) osmiophilic bodies, but in other egress-related vesicles.

Garg *et al.* (2013) showed that an increase in calcium levels is important for EM lysis by PPLP1. Moreover, merozoites secrete more PPLP1 into the medium under high calcium levels, whereas PPLP1 discharge by merozoites was halted in the presence of the calcium chelator BAPTA-AM. Noteworthy, calcium signalling in gametocytes appears to have an effect only after PVM breakdown, because BAPTA-AM is able to inhibit rounding up of the activated gametocytes, but does not prevent PVM rupture (McRobert *et al*., 2008; Sologub *et al*., 2011). In accordance with these findings, we here showed that in the presence of BAPTA-AM PPLP2-containing vesicles do not discharge their content upon gametocyte activation and that in BAPTA-AM-treated activated gametocytes the EC was preserved. These data demonstrate that the discharge of the PPLP2-containing vesicles is dependent on high intracellular calcium levels and occurs after PVM disintegration but before EM rupture.

Gametocytes lacking PPLP2 were unable to egress from erythrocytes and the EC was unable to diffuse from infected erythrocytes after gametocyte activation. Both PPLP2(–) gametocytes and EC were retained within infected erythrocytes and could be easily observed in ultrasections. In the WT, on the other hand, the EC disappears approximately 5 min p.a., thus several minutes before the EM ruptures (Sologub *et al*., 2011). Furthermore, activated PPLP2(–) gametocytes released significantly less haemoglobin into the medium than activated WT gametocytes, suggesting that PPLP2 permeabilizes the EM, resulting in the release of EC into the medium. Noteworthy, treatment of activated gametocytes with E64d and TLCK results in blocked rupture of PVM and EM respectively; however, none of the two protease inhibitors prevents EC release. The combined data suggest that (i) PVM rupture, (ii) EM permeabilization followed by EC release, and (iii) EM rupture are three consecutive but independent events.

Impaired gametogenesis and transmission of PPLP2(–) parasites was rescued by the pore-forming toxin equinatoxin II, while the pore sealant Tetronic 90R4 detained the activated WT gametocytes within the RBC, providing additional evidence for the crucial role of membrane permeabilization in gametocyte egress. In support of this notion, phalloidin influx into activated gametocytes demonstrated that upon gametocyte activation the EM becomes permeable and that permeabilization occurs several minutes before the membrane eventually ruptures. The assays further proved that EM permeabilization is abolished in PPLP2(–) gametocytes. The final piece of evidence on a direct role of PPLP2 in permeabilizing the EM was provided by the fact that recombinant PPLP2 protein is able to lyse RBCs.

In the light of the available data on the molecular mechanism of RBC egress by the malaria gametocyte, we propose the following model (Fig. 9): The mature gametocyte senses environmental stimuli, e.g. xanthurenic acid and a drop in temperature, signalling the transmission from the human to the mosquito. Within approximately 1 min p.a. the osmiophilic bodies discharge egress molecules like GEST or MDV-1/Peg3 into the lumen of the parasitophorous vacuole, resulting in the immediate rupture of the PVM. Upon activation the intracellular calcium levels increase and Pfg377-negative egress vesicles discharge their content, including PPLP2, into the EC. PPLP2 oligomerizes and inserts into the EM thereby forming pores. At approximately 5 min p.a. the EM becomes permeable and the EC is released into the medium, while at the same time the RBC cytoskeleton is weakened by cysteine/serine proteases. The activated gametocyte meanwhile has rounded up and transformed into a gamete. At approximately 10 min p.a., the EM eventually opens by formation of a single pore and releases the fertile gamete into the midgut lumen.

The here presented data, together with the recently published data by Garg *et al.* (2013) and Deligianni *et al.* (2013), provide important evidence for the role of plasmodial perforins in EM permeabilization. The exact mechanism of pore formation and the physiological role of this process, though, remain to be elucidated. PPLP1 was shown to form oligomers as was described for other MACPF proteins (Garg *et al*., 2013). While PF1 of T cells forms mono-oligomeric pre-pores which are then inserted into the target cell membrane causing cytolysis of target cells, the complement components C5b-C8 assemble to form a receptor complex which enables attachment and pore formation by recruitment of C9 components during MAC formation. Interestingly, only C8 alpha-gamma and C9 insert into the target cell membrane (reviewed in Dunstone and Tweten, 2012). Worth mentioning, we detected expression of several *pplps* in the *P. falciparum* blood and gametocyte stages. Thus we hypothesize that the plasmodial perforins may form heteromeres, which might have different compositions dependent on the life cycle stage of the parasite. It is our future goal to determine the detailed mode of action of PPLP2 and its potential interaction with other perforins during RBC egress by activated *P. falciparum* gametocytes.

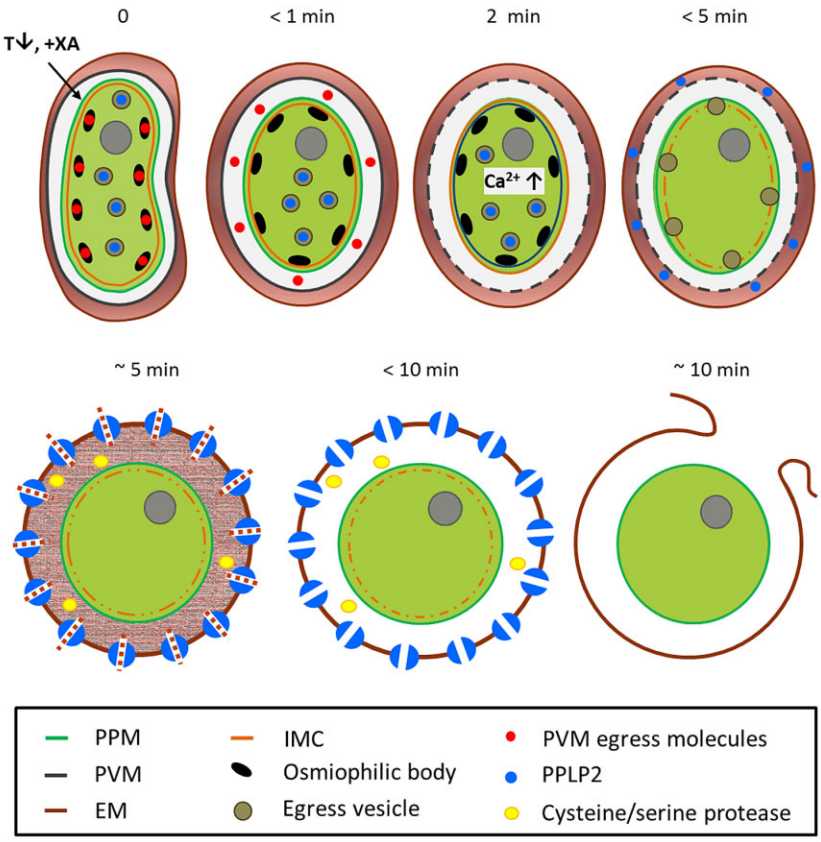

Fig. 9. Hypothetical model of the inside-out egress of activated gametocytes from the RBC. The estimated time lapse is indicated. EM, erythrocyte membrane, IMC, inner membrane complex; PPM, parasite plasma membrane; PVM, parasitophorous vacuole membrane; T, temperature, XA, xanthurenic acid (modified from Wirth and Pradel, 2012).

Experimental procedures

Bioinformatics

The structural representations were generated based on templates discovered by HH-Suite and a pre-prepared PDB library (Soeding, 2005; Remmert *et al.*, 2011). PDB entries 2RD7 (Slade *et al.*, 2008), 3NSJ (Law *et al.*, 2010), 3OJY (Lovelace *et al.*, 2011) and 3T5O (Aleshin *et al.*, 2012) were selected as homology modelling templates. PSIPRED (Jones, 1999) was used to predict the PPLP2 secondary structure from a PSI-BLAST (Altschul *et al.*, 1997) alignment of evolutionary related proteins. Final homology models were designed by the MODELLER (Eswar *et al.*, 2006) software package using multi-template modelling and additional restraints taken from the predicted secondary structure. pGenTHREADER and pDomTHREADER server (Lobley *et al.*, 2009) were used to identify proteins structurally related to the PPLP2 sequence. Missing regions of the full model including N- and C-terminal sites were generated by QUARK online prediction server (Xu and Zhang, 2012) in multiple overlapping structural templates. All parts together with the generated template-based model and secondary structure restraints were structurally concatenated by MODELLER. For the final models generated main-chain and full-atomic energy minimizations were performed by ModRefiner (Xu and Zhang, 2011) in an 8 h run. For structure quality assessment PDBsum server (Laskowski, 2001) was used to inspect Psi/Phi Ramachandran plots. Structural images were generated using PyMOL (The PyMOL Molecular Graphics System, Version 1.6.0.0 Schrödinger, LLC). Protein domain analysis and prediction were performed by SMART (Schultz *et al.*, 1998), CDD (Marchler-Bauer *et al.*, 2013) and PROSITE (Sigrist *et al.*, 2002) online servers.

Parasite culture

Plasmodium falciparum strain NF54 (MR4 MRA-1000, BEI Resources Repository, NIAID, NIH) asexual blood stage parasites and gametocytes were *in vitro* cultivated in human A+ erythrocytes as described (Trager and Jensen, 1976; Ifediba and Vanderberg, 1981). The RPMI1640/Hepes medium (Gibco) was supplemented with 10% heat inactivated human A+ serum or 0.5% AlbuMax II (Gibco), 50 μg ml^{-1} hypoxanthine (Sigma-Aldrich) and 10 μg ml^{-1} gentamicin (Gibco). Human A+ erythrocyte concentrate and serum were purchased from the Department of Transfusion Medicine, University Hospital Aachen, Germany, or obtained from the NIH Department of Transfusion Medicine, USA. The erythrocyte and sera samples were pooled and the donors remained anonymous. For cultivation of PPLP2(–) parasites blasticidin (InvivoGen) was added as selection drug in a final concentration of 5.4 μM, and for cultivation of Pfg377(–) parasites pyrimethamine (Sigma Aldrich) was added in a final concentration of 0.2 μM. All cultures were strictly kept in an atmosphere of 5% O_2, 5% CO_2, and 90% N_2 at 37°C. For synchronization of asexual blood stages, parasite cultures with 3–4% ring stages were centrifuged to obtain the pellet, which was resuspended in five times pellet's volume of prewarmed 5% sorbitol (AppliChem) in RPMI medium (Invitrogen) and incubated at room temperature (RT) for 10 min (Lambros and Vanderberg, 1979). The cells were washed once with RPMI medium to

remove the sorbitol, diluted to 5% vol. hematocrit and cultured as described above. For the experiments with asexual parasites, schizonts were isolated from infected cultures using a Percoll enrichment protocol and used to initiate a new 2 h time span synchronized infection in erythrocytes from the same donor blood drawn within 2 days of the procedure. Between 40 and 50 h after synchronized culture initiation, cells were subjected to experimentation. Gametocytes were enriched via Percoll gradient (GE Healthcare Life Sciences) as previously described (Kariuki *et al*., 1998). Gametogenesis was induced by incubating mature gametocyte cultures in 100 μM xanthurenic acid (XA) for 15 min at RT (Billker *et al*., 1998; Garcia *et al*., 1998).

Mosquito maintenance

An. stephensi mosquitoes were reared under standard insectary conditions at 26 ± 0.5°C, 80 ± 2% humidity and a 12/12 h light/dark cycle. Production of eggs was induced by feeding adult female mosquitoes with non-infected human blood, and four days later eggs were collected on filter paper in a beaker containing 0.1% sea salt solution. Following emergence of larvae, these were reared at a fixed density of 300 larvae per 3 l tray in 0.1% sea salt solution. Larvae were fed on fodder pellets. Pupae were collected following transformation and placed in cages for mosquito emergence. Adult mosquitoes were fed via a pad soaked with 5% sterile saccharose solution supplemented with para-aminobenzoic acid (PABA).

Recombinant protein expression

Two recombinant peptides, PPLP2RP1 and PPLP2RP2 (see Fig. 1A for domains), were expressed as fusion proteins with an N-terminal maltose binding protein (MBP)-tag to be used for the immunization of mice. Gene fragments were amplified from *P. falciparum* genomic DNA using PPLP2RP1 forward primer 5′-ATGAATTCGGTGATAAACGTTCAAAGGAAA-3′ and PPLP2RP1 reverse primer 5′-TAGAATTCTTAGGAAAATCCCA TTAATATCGTTG-3′ as well as PPLP2RP2 forward primer 5′-GCGTAAGGCCTTCAAGCGCTTTTCAAAAAGAAGCA-3′ and PPLP2RP2 reverse primer 5′-TACGCGTCGACTTATCTGGTT GCTTGAAAATTTGTATG-3′, resulting in gene fragments of 1020 and 948 bp respectively. Cloning into the pIH-vector was mediated by EcoRI and SalI/StuI restriction sites (underlined) respectively. Recombinant proteins were expressed in *E. coli* BL21 (DE3) RIL cells according to the manufacturer's protocol (Stratagene). The MBP-tagged fusion proteins were affinity-purified via amylose resin (New England Biolabs) as previously described (Williamson *et al*., 1995) with following modifications of the procedure: pelleted bacteria were directly resuspended in lysis buffer containing complete, EDTA-free protease inhibitor cocktail (Roche), incubated on ice for 20 min and homogenized by 4 min sonication (50 cycles/50% intensity). DNase treatment was not deployed. Amylose-bound fusion protein was eluted during batch purification according to the manufacturer's manual. A gene fragment encoding for full length PPLP2 (PPLP2RP3, excluding the signal sequence; see Fig. 1A) was cloned into the mammalian expression vector pRADU, adjacent to a mammalian secretory signal sequence. For expression of His-tagged PPLP2RP3, mammalian Human Embryonic Kidney 293 cells (HEK-293) were used. HEK-293 cells were cultured in Dulbecco Modified Eagle Medium (DMEM; Invitrogen, USA) with 10% heat-inactivated fetal calf serum (FCS) in a humidified CO_2 (5%) incubator at 37°C. Fresh monolayers of 60% to 70% confluent HEK-293 cells were transfected with the expression vector using jetPRIME reagent according to manufacturer's protocol (Hichem Life Sciences). After 48 h, the supernatant of transfected HEK-293 cells containing secreted protein was harvested and used for purification of PPLP2RP3 by Ni-NTA chromatography. The purified PPLP2RP3 was analysed by Western blotting and Silver staining as previously described (Garg *et al*., 2013) and used to test the haemolytic activity via erythrocyte lysis assays.

Generation of antisera

MBP-tagged PPLP2RP1 and PPLP2RP2 peptides were purified via affinity chromatography as described above and PBS buffer exchange was performed via filter centrifugation with Amicon Ultra 15 centrifugal filter units (Sigma Aldrich) according to manufacturer's protocol. Polyclonal immune sera were generated by immunization of 6 weeks old female NMRI mice (Charles River Laboratories) with subcutaneous injections of 100 μg recombinant protein emulsified in Freund's incomplete adjuvant (Sigma-Aldrich). Two boosts of 30 μg protein followed in week 4 and week 5. Mice were anesthetized at day 5 after the second boost by intraperitoneal injection of a mixture of ketamine and xylazine according to the manufacturer's protocol (Sigma-Aldrich), and immune sera were collected via heart puncture. Following sera collection the anesthetized mice were sacrificed via severing the cervical spine. The immune sera of three mice immunized with the same antigen were pooled; sera of three non-immunized mice were used as negative control. The antisera recognized the cognate recombinant protein (data not shown). Experiments for the generation of antisera in mice were approved by the animal welfare committees of the government of Lower Franconia, Germany (ref. no. 55.2–2531.01–58/09) and of the District Council of Cologne, Germany (ref. no. 84-02.05.30.12.097 TVA).

Diagnostic RT-PCR

Trophozoites and schizonts of synchronized NF54 cultures were harvested and immature gametocytes (stage II-IV) and non-activated mature gametocytes were enriched by Percoll gradient purification. Total RNA was isolated using the Trizol reagent (Invitrogen) according to the manufacturer's protocol. RNA preparations were treated with RNase-free DNase I (Qiagen) to remove genomic DNA contamination, followed by phenol/chloroform extraction and ethanol precipitation. All RNA samples had A260/A280 ratios higher than 2.1. Two micrograms of each total RNA sample were used for cDNA synthesis using the SuperScript III First-Strand Synthesis System (Invitrogen), following the manufacturer's instructions. Transcript for *pplp2* was amplified with PPLP2RT1 forward primer 5′-AGTAGTACAA CAAGGAGAAG-3′ and PPLP2RT1 reverse primer 5′-CTGATA TAACATCACCTAAA-3′, using a PCR cycle number of 25. Controls without reverse transcriptase were used to investigate potential genomic DNA contamination by diagnostic PCR using *pfaldolase*-specific primers (AldolaseRT1 forward primer 5′-TAGATGGATTAGCAGAAAGATGC-3′; AldolaseRT1 reverse

primer 5′-AGAAACCAACCATCTTGAGTAGTGG-3′). RNA quality was further verified for stage specificity by monitoring transcripts of the blood stage-specific gene *ama1* and the gametocyte-specific gene *pfccp2* (Ama1RT1 forward primer 5′-GGATTATGGGTCGATGGA-3′; Ama1RT1 reverse primer 5′-GATCATACTAGCGTTCTT-3′; PfCCp2RT1 forward primer 5′-TCGGATGGAGAATCCGTT-3′; PfCCp2RT1 reverse primer 5′-GTATCCCATGTCTTGTGA-3′). Transcript analysis for *pfaldolase* was used for loading control.

Indirect immunofluorescence assay

Parasite preparations for IFAs included mixed NF54 WT or PPLP2(–) asexual blood stages or mature NF54 WT gametocytes as well as mature gametocytes of a previously described Pfg377(–) line (de Koning-Ward *et al.*, 2008) and of the PPLP2(–) line. For the egress studies, mature NF54 WT gametocytes were activated with 100 μM XA at RT and samples were taken at 2, 10 and 15 min p.a. For studies of the effect of BAPTA-AM (Santa Cruz Biotechnology) on the localization of PPLP2 during gametocyte activation, mature gametocytes were pre-incubated with BAPTA-AM in a final concentration of 25 μM for 15 min at 37°C. The cultures were subsequently activated and samples were taken at 0, 5, 10 and 20 min p.a. As a negative control gametocytes from the same culture were treated with the same volume of the solvent DMSO (Dimethylsulfoxide; Sigma Aldrich). Monolayers of infected erythrocytes were air dried on slides and fixed for 10 min with 4% paraformaldehyde (pH 7.4). For membrane permeabilization and blocking of non-specific binding, preparations were permeabilized with 0.1% vol. Triton X-100 and 125 mM glycine (Carl Roth) in PBS for 30 min, followed by blocking with 3% BSA in PBS for 1 h. Preparations were then incubated with anti-PPLP2 mouse antisera at 37°C for 2 h. Binding of primary antibody was visualized by incubating the preparations with fluorophore-conjugated goat anti-mouse antibodies (Alexa Fluor 488; Molecular Probes) at RT for 1 h. Asexual blood stage parasites were highlighted with rabbit immune sera specific for MSP1 (ATCC), while gametocytes were highlighted with rabbit anti-Pfs230 or anti-Pfs25 antisera, followed by incubation with fluorophore-conjugated goat anti-rabbit antibodies (Alexa Fluor 594; Molecular Probes). Nuclei were highlighted by incubating the specimens with Hoechst nuclear stain 33342 (Molecular Probes) for 1 min. Labelled specimens were examined using an Olympus BX41 fluorescence microscope in combination with a ProgRes Speed XT5 camera with the exception of Fig. S1C and D, which were taken by a Leica DM5500 B fluorescence microscope. Digital images were processed using Adobe Photoshop CS software.

Generation of PPLP2(–) parasites

Gene-disruptant PPLP2(–) parasites were generated by single homologous cross-over recombination using the disruption vector pCAM-BSD (Dorin-Semblat *et al.*, 2007; Simon *et al.*, 2009). A 802 bp gene fragment homologous to a region within the MACPF domain of *pplp2* (see Fig. 3A) was amplified by PCR, using PPLP2KO1 forward primer 5′-TAGGATCCTTGTCTCTTAAGTATTTAGGTTTAGGA-3′ and PPLP2KO1 reverse primer 5′-ATGCGGCCGCTTATATTTCATATGCAACATGTGTACC-3′. Cloning into pCAM-BSD was mediated by BamHI and NotI restriction sites (underlined). A NF54 WT culture with 4% ring stages was loaded with 60 μg of the disruption vector in transfection buffer via electroporation (parameters: 310 V 950 μF, 13 ms; Bio-Rad gene-pulser) as described (Sidhu *et al.*, 2005). Blasticidin (InvivoGen) was added to a final concentration of 5.4 μM, starting at 4 h after transfection. A mock control was electroporated using transfection buffer without the disruption vector and cultured in regular medium. Blasticidin-resistant parasites appeared after 3–4 weeks. After 60–90 days of drug pressure, the respective cultures were investigated for plasmid-integration by diagnostic PCR. DNA of the transfected parasites was isolated using NucleoSpin Blood (Macherey-Nagel) according to the manufacturer's protocol and used as template in the diagnostic PCR. The following primers were used to test for vector integration: PPLP2KO-5′ integration forward primer 5′-GGAAGGGGCATAAGAAGAAGA-3′, PPLP2KO-3′ integration reverse primer 5′-GCGCTTGATAATCCCATCTT-3′, pCAM-BSD forward primer 5′-TATTCCTAATCATGTAAATCTTAAA-3′ and pCAM-BSD reverse primer 5′-CAATTAACCCTCACTAAAG-3′. Vector integration was confirmed by sequencing using PPLP2KO-5′ Integration forward primer (Sequence 1), PPLP2KO-3′ Integration reverse primer (Sequence 3), pCAM-BSD forward primer (Sequence 4) and pCAM-BSD Seq reverse primer 5′-ACGCAATTAATGTGAGTTAG-3′ (Sequence 2; Fig. S7; Fraunhofer IME Aachen).

Parasite replication, erythrocyte invasion and parasite egress assay

Synchronized cultures were prepared as described above. Cultures were maintained for 3–7 days at 1% hematocrit. After ~ 18 h in culture, the parasitemia of NF54 WT and PPLP2(–) cultures was adjusted by addition of uninfected erythrocytes with the preservation of culture hematocrit. After ~ 72 h and 7 days, in culture respectively, the parasitemia was assessed using the acridine orange method in 600–1500 cells. The parasite egress assay was used to evaluate the length of erythrocytic cycle. The detailed description of the parasite egress assay is published (Glushakova *et al.*, 2007). Briefly, cells infected with NF54 WT or PPLP2(–) parasites were injected into environmental chambers for microscopy (HybriWell HBW20, Grace Bio-Labs, Bend, OR) at 0.25% hematocrit at consecutive time points, every 2 h spanning 40–52 h of the erythrocyte cycle, incubated at 37°C to accumulate 'sites of parasite egress', and then cooled in chambers to 15°C to stop parasite egress. Egress was calculated as the fraction of schizonts that ruptured and formed 'egress sites' composed of scattered merozoites in the chamber (Fig. 4D) during the incubation time. To assess the effect of Tetronic 90R4 on merozoite egress, NF54 WT and PPLP2(–) schizonts were resuspended in the medium supplemented with 0.5% AlbuMax and Tetronic 90R4 (Ethylenediamine tetrakis(ethoxylate-block-propoxylate) tetrol; Sigma Aldrich) at concentrations of 10, 20 and 30 mg ml^{-1}, and kept for 1 h at 37°C in the environmental chambers to accumulate sites of parasite egress. Egress was assessed by light microscopy and calculated as a fraction of schizonts that finished the replication cycle and released merozoites during the incubation time. Results are presented as mean ± SEM of three independent experiments for NF54 WT parasites. One experiment was performed with PPLP2(–) parasites to confirm Tetronic 90R4 effect on egress observed with WT parasites. A total of 300–1000 schizonts per sites of egress were counted for each experimental condition.

Live cell microscopy

DIC light microscopy (LSM 510, Zeiss; 63× 1.4 NA oil objectives) was used for live-cell analysis of infected cells in the chambers for egress assay. A laser scanning microscope was used to record images with a 63× 1.4 NA oil objective and laser excitation at 488 nm. A laser excitation at 633 nm with a low intensity of cell illumination to avoid photodamage of schizonts was used for time-lapse recordings of parasite egress from and parasite invasion into erythrocytes. To detect the cytoskeleton protein F-actin, a fluorescent phalloidin (~ 100 nM) (Alexa Fluor 488® phalloidin, Invitrogen) was used as described before (Glushakova *et al.*, 2010). The fluorescent phalloidin was excited with a 488 nm laser at low intensity of light.

Exflagellation assay

A volume of 100 µl of a mature gametocyte culture [NF54 WT or PPLP2(–)] was activated by incubation with 100 µM XA for 15 min at RT. To test the effect of the pore sealant Tetronic 90R4 on exflagellation, 100 µl of a mature NF54 WT gametocyte culture was incubated for 1 h at 37°C with Tetronic 90R4 in concentrations of 5, 10, 20 and 30 mg ml^{-1}. As a negative control gametocytes were pre-incubated with the corresponding volume of deionized water. At 15 min p.a., exflagellation centres were counted at 400-fold magnification in 30 optical fields using a Leica DMLS microscope. Three independent experiments were performed in duplicates and exflagellation was calculated as a percentage of the number of exflagellation centres in the Tetronic 90R4-treated or PPLP2(–) culture in relation to the number of exflagellation centres in untreated WT control (set to 100%).

Microgamete quantification

In order to assess the formation of microgametes after artificial removal of the EM, mature NF54 WT and PPLP2(–) gametocytes were incubated either with 0.05 mg ml^{-1} equinatoxin II (kindly provided by G. Anderluh, University of Ljubljana) in culture medium or in culture medium alone (control) for 10 min at 37°C. After washing with culture medium the gametocytes were activated by 100 µM XA at RT. At 20 min p.a. samples were taken and subjected to IFA. The sexual stage parasites were highlighted by Pfs230-labelling, followed by staining of nuclei as described above. The numbers of microgametes in relation to all Pfs230-positive parasites were counted at 630-fold magnification in 30 optical fields in triplicate using a Zeiss Axiolab fluorescence microscope.

Transmission electron microscopy

Mature gametocyte cultures of line PPLP2(–) or of NF54 WT were activated with 100 µM XA at RT and samples were collected at 0, 7, 15 and 30 min p.a. Cell samples were fixed in 1% glutaraldehyde and 4% paraformaldehyde in PBS (pH 7.4) over night at 4°C. In the case of protease inhibitor treatment, Percoll-enriched gametocytes in a volume of 100 µl were pre-incubated for 15 min at 37°C with the respective inhibitor at the following inhibitory concentrations: TLCK, 100 µM; E-64d, 1 mM; 1,10-phenanthroline, 1 mM. Samples were activated, collected at 30 min, and fixed as described above. The specimens were post-fixed in 1% osmium tetroxide and 1.5% $K_3Fe(CN)_6$ in PBS for 2 h at RT, followed by incubation in 0.5% uranyl acetate for 1 h. The fixed specimens were dehydrated in increasing concentrations of ethanol (70%/80%/95%/100%) and then incubated for 1 h in propylene oxide, followed by another incubation step for 1 h in a 1:1 mixture of propylene oxide and Epon (Sigma Aldrich). Specimens were subsequently embedded in Epon at 60°C for 2 days. Ultrasections were cut with a Leica ultramicrotome Ultracut UCT and post-stained with 1% uranyl acetate for 30 min and 0.2% lead citrate for 15 s. Sections were examined with a CM100 transmission electron microscope (FEI). The images were recorded digitally with a Quemesa TEM CCD camera and iTEM software (Olympus Soft Imaging Solutions). Alternatively, samples were analysed with a Zeiss EM10 transmission electron microscope and the photographs taken were scanned and processed using Adobe Photoshop CS software.

Standard membrane feeding assay

An. stephensi mosquitoes were fed with a 5% sterile saccharose solution supplemented with PABA and 40 µg ml^{-1} gentamicin until the assay was performed (Beier *et al.*, 1994). Mature NF54 WT and PPLP2(–) gametocytes, positively tested for exflagellation activity were enriched via Percoll gradient (GE Healthcare Life Sciences) as previously described (Kariuki *et al.*, 1998) and quantified using a Neubauer chamber. The parasite-to-non-infected erythrocyte ratio was set to 0.25%. The cell suspension was fed to the mosquitoes via glass feeders and the mosquitoes were allowed to feed for 20 min (Bishop and Gilchrist, 1946). At 10 days post feeding, midguts of mosquitoes which took a blood meal were dissected and stained with 0.2% mercurochrome in PBS. The numbers of oocysts per midgut were counted under the microscope. In case of equinatoxin II treatment, gametocytes were incubated either with 0.05 mg ml^{-1} equinatoxin II in culture medium or in culture medium alone (control) for 10 min at 37°C after purification via Percoll gradient. After washing with culture medium, the parasite-to-non infected erythrocyte ratio was set to 0.25% and fed to mosquitoes as described above. Data analysis was performed using GraphPad Prism program version 5.

Haemoglobin release assay

The gametocytemia of mature NF54 WT or PPLP2(–) gametocyte cultures positively tested for exflagellation activity was determined using a Neubauer chamber and used to calculate the culture volume containing 2×10^5 mature gametocytes. For the assay the calculated volume of cell suspension was aliquoted, washed twice with cell culture medium to remove excess haemoglobin and filled in a 96-well-plate with a final volume of 100 µl per well in triplicate. The gametocytes were activated with 100 µM XA at RT. At 45 min p.a., the cells were pelleted by mild centrifugation and 60 µl supernatant of each sample were transferred to another 96-well-plate to measure its optical density at OD_{405} using Multimode Reader infinite200 (Tecan). The supernatant of non-activated gametocytes was set to 0% and of RBCs completely lysed using 0.1% saponin/PBS was set to 100%.

Erythrocyte lysis assay

Human erythrocytes were washed in lysis buffer (150 mM NaCl, 1 mM $CaCl_2$, and 20 mM Hepes pH 7.2) and counted in a

haemocytometer. A total number of 5×10^6 human erythrocytes were resuspended in 50 µl lysis buffer with different concentration of PPLP2RP3 ranging between 0–40 nM in triplicate and further incubated for 30 min at 37°C. The release of haemoglobin into the supernatant following lysis was estimated by measuring the absorbance at OD_{405}. Erythrocyte lysis was expressed as a percentage of maximum haemoglobin release compared with 100% lysis of 5×10^6 human RBCs by suspension in water.

Acknowledgements

We thank Inga Siden-Kiamos (FORTH Institute of Molecular Biology and Biotechnology Crete) for helpful discussions. We are grateful to Gregor Anderluh (University of Ljubljana) for providing equinatoxin II, to Pietro Alano (Istituto Superiore di Sanità Rome) for providing parasite line Pfg377(–) and to Kim Williamson (Loyola University Chicago) for providing vector pIH. We further thank the team of Georg Krohne (University of Würzburg) and the Electron Microscopy Unit for Biological Sciences (University of Oslo) for support with the electron microscopy-related work. The authors acknowledge funding by the priority programme SPP1580 of the Deutsche Forschungsgemeinschaft (G.P. and G.G.).

References

Alano, P., Read, D., Bruce, M., Aikawa, M., Kaido, T., Tegoshi, T., *et al.* (1995) COS cell expression cloning of Pfg377, a *Plasmodium falciparum* gametocyte antigen associated with osmiophilic bodies. *Mol Biochem Parasitol* **74:** 143–156.

Aleshin, A.E., Schraufstatter, I.U., Stec, B., Bankston, L.A., Liddington, R.C., and DiScipio, R.G. (2012) Structure of complement C6 suggests a mechanism for initiation and unidirectional, sequential assembly of membrane attack complex (MAC). *J Biol Chem* **287:** 10210–10222.

Altschul, S.F., Madden, T.L., Schäffer, A.A., Zhang, J., Zhang, Z., Miller, W., and Lipman, D.J. (1997) Gapped BLAST and PSI-BLAST: a new generation of protein database search programs. *Nucleic Acids Res* **25:** 3389–3402.

Baum, J., Gilberger, T.W., Frischknecht, F., and Meissner, M. (2008) Host-cell invasion by malaria parasites: insights from *Plasmodium* and *Toxoplasma*. *Trends Parasitol* **24:** 557–563.

Beier, M.S., Pumpuni, C.B., Beier, J.C., and Davis, J.R. (1994) Effects of para-aminobenzoic acid, insulin, and gentamicin on *Plasmodium falciparum* development in anopheline mosquitoes (Diptera: Culicidae). *J Med Entomol* **31:** 561–565.

Billker, O., Lindo, V., Panico, M., Etienne, A.E., Paxton, T., Dell, A., *et al.* (1998) Identification of xanthurenic acid as the putative inducer of malaria development in the mosquito. *Nature* **392:** 289–292.

Bishop, A., and Gilchrist, B.M. (1946) Experiments upon the feeding of *Aedes aegypti* through animal membranes with a view to applying this method to the chemotherapy of malaria. *Parasitology* **37:** 85–100.

Chandramohanadas, R., Davis, P.H., Beiting, D.P., Harbut, M.B., Darling, C., Velmourougane, G., *et al.* (2009) Apicomplexan parasites co-opt host calpains to facilitate their escape from infected cells. *Science* **324:** 794–797.

Chandramohanadas, R., Park, Y., Lui, L., Li, A., Quinn, D., Liew, K., *et al.* (2011) Biophysics of malarial parasite exit from infected erythrocytes. *PLoS ONE* **6:** e20869.

de Koning-Ward, T.F., Olivieri, A., Bertuccini, L., Hood, A., Silvestrini, F., Charvalias, K., *et al.* (2008) The role of osmiophilic bodies and Pfg377 expression in female gametocyte emergence and mosquito infectivity in the human malaria parasite *Plasmodium falciparum*. *Mol Microbiol* **67:** 278–290.

Deligianni, E., Morgan, R.N., Bertuccini, L., Wirth, C.C., Silmon de Monerri, N.C., Spanos, L., *et al.* (2013) A perforin-like protein mediates disruption of the erythrocyte membrane during egress of *Plasmodium berghei* male gametocytes. *Cell Microbiol* **15:** 1438–1455.

Delves, M.J., Ruecker, A., Straschil, U., Lelièvre, J., Marques, S., López-Barragán, M.J., *et al.* (2013) Male and female *Plasmodium falciparum* mature gametocytes show different responses to antimalarial drugs. *Antimicrob Agents Chemother* **57:** 3268–3274.

Dorin-Semblat, D., Quashie, N., Halbert, J., Sicard, A., Doerig, C., Peat, E., *et al.* (2007) Functional characterization of both MAP kinases of the human malaria parasite *Plasmodium falciparum* by reverse genetic. *Mol Microbiol* **65:** 1170–1180.

Dunstone, M.A., and Tweten, R.K. (2012) Packing a punch: the mechanism of pore formation by cholesterol dependent cytolysins and Membrane Attack/Perforin-like proteins. *Curr Opin Struct Biol* **22:** 342–349.

Ecker, A., Pinto, S.B., Baker, K.W., Kafatos, F.C., and Sinden, R.E. (2007) *Plasmodium berghei*: *Plasmodium* perforin-like protein 5 is required for mosquito midgut invasion in *Anopheles stephensi*. *Exp Parasitol* **116:** 504–508.

Eswar, N., Marti-Renom, M.A., Webb, B., Madhusudhan, M.S., Eramian, D., Shen, M., *et al.* (2006) Comparative protein structure modeling with MODELLER. *Curr Protoc Bioinformatics* **Chapter 5:** Unit 5.6.

Furuya, T., Mu, J., Hayton, K., Liu, A., Duan, J., Nkrumah, L., *et al.* (2005) Disruption of a *Plasmodium falciparum* gene linked to male sexual development causes early arrest in gametocytogenesis. *Proc Natl Acad Sci USA* **102:** 16813–16818.

Garcia, G.E., Wirtz, R.A., Barr, J.R., Woolfitt, A., and Rosenberg, R. (1998) Xanthurenic acid induces gametogenesis in *Plasmodium*, the malaria parasite. *J Biol Chem* **273:** 12003–12005.

Garg, S., Agarwal, S., Kumar, S., Yazdani, S.S., Chitnis, C.E., and Singh, S. (2013) Calcium-dependent permeabilization of erythrocytes by a perforin-like protein during egress of malaria parasites. *Nat Commun* **4:** 1736.

Glushakova, S., Yin, D., Li, T., and Zimmerberg, J. (2005) Membrane transformation during malaria parasite release from human red blood cells. *Curr Biol* **15:** 1645–1650.

Glushakova, S., Yin, D., Gartner, N., and Zimmerberg, J. (2007) Quantification of malaria parasite release from infected erythrocytes: inhibition by protein-free media. *Malar J* **6:** 61.

Glushakova, S., Mazar, J., Hohmann-Marriott, M.F., Hama,

E., and Zimmerberg, J. (2009) Irreversible effect of cysteine protease inhibitors on the release of malaria parasites from infected erythrocytes. *Cell Microbiol* **11:** 95–105.

Glushakova, S., Humphrey, G., Leikina, E., Balaban, A., Miller, J., and Zimmerberg, J. (2010) New stages in the program of malaria parasite egress imaged in normal and sickle erythrocytes. *Curr Biol* **20:** 1117–1121.

Glushakova, S., Lizunov, V., Blank, P.S., Melikov, K., Humphrey, G., and Zimmerberg, J. (2013) Cytoplasmic free Ca^{2+} is essential for multiple steps in malaria parasite egress from infected erythrocytes. *Malar J* **12:** 41.

Graewe, S., Rankin, K.E., Lehmann, C., Deschermeier, C., Hecht, L., Froehlke, U., *et al.* (2011) Hostile takeover by *Plasmodium*: reorganization of parasite and host cell membranes during liver stage egress. *PLoS Pathog* **7:** e1002224.

Grüring, C., Heiber, A., Kruse, F., Ungefehr, J., Gilberger, T.W., and Spielmann, T. (2011) Development and host cell modifications of *Plasmodium falciparum* blood stages in four dimensions. *Nat Commun* **2:** 165.

Hall, R., Hyde, J.E., Goman, M., Simmons, D.L., Hope, I.A., Mackay, M., *et al.* (1984) Major surface antigen gene of a human malaria parasite cloned and expressed in bacteria. *Nature* **311:** 379–382.

Ifediba, T., and Vanderberg, J.P. (1981) Complete *in vitro* maturation of *P. falciparum* gametocytes. *Nature* **294:** 364–366.

Ishino, T., Chinzei, Y., and Yuda, M. (2005) A *Plasmodium* sporozoite protein with a membrane attack complex domain is required for breaching the liver sinusoidal cell layer prior to hepatocyte infection. *Cell Microbiol* **7:** 199–208.

Jackson, K.E., Spielmann, T., Hanssen, E., Adisa, A., Separovic, F., Dixon, M.W., *et al.* (2007) Selective permeabilization of the host cell membrane of *Plasmodium falciparum*-infected red blood cells with streptolysin O and equinatoxin II. *Biochem J* **403:** 167–175.

Jones, D.T. (1999) Protein secondary structure prediction based on position-specific scoring matrices. *J Mol Biol* **292:** 195–202.

Kadota, K., Ishino, T., Matsuyama, T., Chinzei, Y., and Yuda, M. (2004) Essential role of membrane-attack protein in malarial transmission to mosquito host. *Proc Natl Acad Sci USA* **101:** 16310–16315.

Kafsack, B.F., and Carruthers, V.B. (2010) Apicomplexan perforin-like proteins. *Commun Integr Biol* **3:** 18–23.

Kaiser, K., Camargo, N., Coppens, I., Morrisey, J.M., Vaidya, A.B., and Kappe, S.H. (2004) A member of a conserved *Plasmodium* protein family with membrane-attack complex/perforin (MACPF)-like domains localizes to the micronemes of sporozoites. *Mol Biochem Parasitol* **133:** 15–26.

Kariuki, M.M., Kiaira, J.K., Mulaa, F.K., Mwangi, J.K., Wasunna, M.K., and Martin, S.K. (1998) *Plasmodium falciparum*: purification of the various gametocyte developmental stages from *in vitro*-cultivated parasites. *Am J Trop Med Hyg* **59:** 505–508.

Knapp, B., Hundt, E., and Kiipper, H.A. (1990) *Plasmodium falciparum* aldolase: gene structure and localization. *Mol Biochem Parasitol* **40:** 1–12.

Lambros, C., and Vanderberg, J.P. (1979) Synchronization of *Plasmodium falciparum* erythrocytic stages in culture. *J Parasitol* **65:** 418–420.

Lanfrancotti, A., Bertuccini, L., Silvestrini, F., and Alano, P. (2007) *Plasmodium falciparum*: mRNA co-expression and protein co-localisation of two gene products upregulated in early gametocytes. *Exp Parasitol* **116:** 497–503.

Laskowski, R.A. (2001) PDBsum: summaries and analyses of PDB structures. *Nucleic Acids Res* **29:** 221–222.

Law, R.H.P., Lukoyanova, N., Voskoboinik, I., Caradoc-Davies, T.T., Baran, K., Dunstone, M.A., *et al.* (2010) The structural basis for membrane binding and pore formation by lymphocyte perforin. *Nature* **468:** 447–451.

Lobley, A., Sadowski, M.I., and Jones, D.T. (2009) pGenTHREADER and pDomTHREADER: new methods for improved protein fold recognition and superfamily discrimination. *Bioinformatics* **25:** 1761–1767.

Lovelace, L.L., Cooper, C.L., Sodetz, J.M., and Lebioda, L. (2011) Structure of human C8 protein provides mechanistic insight into membrane pore formation by complement. *J Biol Chem* **286:** 17585–17592.

McRobert, L., Taylor, C.J., Deng, W., Fivelman, Q.L., Cummings, R.M., Polley, S.D., *et al.* (2008) Gametogenesis in malaria parasites is mediated by the cGMP-dependent protein kinase. *PLoS Biol* **6:** e139.

Marchler-Bauer, A., Zheng, C., Chitsaz, F., Derbyshire, M.K., Geer, L.Y., Geer, R.C., *et al.* (2013) CDD: conserved domains and protein three-dimensional structure. *Nucleic Acids Res* **41:** D348–D352.

Peterson, M.G., Marshall, V.M., Smythe, J.A., Crewther, P.E., Lew, A., Silva, A., *et al.* (1989) Integral membrane protein located in the apical complex of *Plasmodium falciparum*. *Mol Cell Biol* **9:** 3151–3154.

Ponzi, M., Siden-Kiamos, I., Bertuccini, L., Curra, C., Kroeze, H., Camarda, G., *et al.* (2009) Egress of *Plasmodium berghei* gametes from their host erythrocyte is mediated by the MDV-1/PEG3 protein. *Cell Microbiol* **11:** 1272–1288.

Pradel, G. (2007) Proteins of the malaria parasite sexual stages: expression, function and potential for transmission blocking strategies. *Parasitology* **134:** 1911–1929.

Pradel, G., Hayton, K., Aravind, L., Iyer, L.M., Abrahamsen, M.S., Bonawitz, A., *et al.* (2004) A multidomain adhesion protein family expressed in *Plasmodium falciparum* is essential for transmission to the mosquito. *J Exp Med* **199:** 1533–1544.

Regev-Rudzki, N., Wilson, D.W., Carvalho, T.G., Sisquella, X., Coleman, B.M., Rug, M., *et al.* (2013) Cell-cell communication between malaria-infected red blood cells via exosome-like vesicles. *Cell* **153:** 1120–1133.

Remmert, M., Biegert, A., Hauser, A., and Soeding, J. (2011) HHblits: lightning-fast iterative protein sequence searching by HMM-HMM alignment. *Nat Methods* **9:** 173–175.

Roiko, M.S., and Carruthers, V.B. (2009) New roles for perforins and proteases in apicomplexan egress. *Cell Microbiol* **11:** 1444–1452.

Rosado, C.J., Kondos, S., Bull, T.E., Kuiper, M.J., Law, R.H.P., Buckle, A.M., *et al.* (2008) The MACPF/CDC family of pore-forming toxins. *Cell Microbiol* **10:** 1765–1774.

Schultz, J., Milpetz, F., Bork, P., and Ponting, C.P. (1998) SMART, a simple modular architecture research tool: identification of signaling domains. *Proc Natl Acad Sci USA* **95:** 5857–5864.

Severini, C., Silvestrini, F., Sannella, A., Barca, S., Gradoni, L., and Alano, P. (1999) The production of the osmiophilic body protein Pfg377 is associated with stage of maturation and sex in *Plasmodium falciparum* gametocytes. *Mol Biochem Parasitol* **100:** 247–252.

Sidhu, A.B.S., Valderramos, S.G., and Fidock, D.A. (2005) pfmdr1 mutations contribute to quinine resistance and enhance mefloquine and artemisinin sensitivity in *Plasmodium falciparum*. *Mol Microbiol* **57:** 913–926.

Sigrist, C.J.A., Cerutti, L., Hulo, N., Gattiker, A., Falquet, L., Pagni, M., *et al.* (2002) PROSITE: a documented database using patterns and profiles as motif descriptors. *Brief Bioinform* **3:** 265–274.

Silvestrini, F., Bozdech, Z., Lanfrancotti, A., Di Giulio, E., Bultrini, E., Picci, L., *et al.* (2005) Genome-wide identification of genes upregulated at the onset of gametocytogenesis in *Plasmodium falciparum*. *Mol Biochem Parasitol* **143:** 100–110.

Simon, N., Scholz, S.M., Moreira, C.K., Templeton, T.J., Kuehn, A., Dude, M.A., and Pradel, G. (2009) Sexual stage adhesion proteins form multi-protein complexes in the malaria parasite *Plasmodium falciparum*. *J Biol Chem* **284:** 14537–14546.

Simon, N., Lasonder, E., Scheuermayer, M., Kuehn, A., Tews, S., Fischer, R., *et al.* (2013) Malaria parasites co-opt human factor H to prevent complement-mediated lysis in the mosquito midgut. *Cell Host Microbe* **13:** 29–41.

Sinden, R.E. (1982) Gametocytogenesis of *Plasmodium falciparum in vitro*: an electron microscopic study. *Parasitology* **84:** 1–11.

Sinden, R.E., Canning, E.U., and Spain, B. (1976) Gametogenesis and fertilization in *Plasmodium yoelii nigeriensis*: a transmission electron microscope study. *Proc R Soc Lond B Biol Sci* **193:** 55–76.

Slade, D.J., Lovelace, L.L., Chruszcz, M., Minor, W., Lebioda, L., and Sodetz, J.M. (2008) Crystal structure of the MACPF domain of human complement protein C8α in complex with the C8γ subunit. *J Mol Biol* **379:** 331–342.

Soeding, J. (2005) Protein homology detection by HMM-HMM comparison. *Bioinformatics* **21:** 951–960.

Sologub, L., Kuehn, A., Kern, S., Przyborski, J., Schillig, R., and Pradel, G. (2011) Malaria proteases mediate inside-out egress of gametocytes from red blood cells following parasite transmission to the mosquito. *Cell Microbiol* **13:** 897–912.

Talman, A.M., Lacroix, C., Marques, S.R., Blagborough, A.M., Carzaniga, R., Ménard, R., and Sinden, R.E. (2011) PbGEST mediates malaria transmission to both mosquito and vertebrate host. *Mol Microbiol* **82:** 462–474.

Trager, W., and Jensen, J.B. (1976) Human malaria parasites in continuous culture. *Science* **193:** 673–675.

Voskoboinik, I., Thia, M.C., Fletcher, J., Ciccone, A., Browne, K., Smyth, M.J., and Trapani, J.A. (2005) Calcium-dependent plasma membrane binding and cell lysis by perforin are mediated through its C2 domain: a critical role for aspartate residues 429, 435, 483, and 485 but not 491. *J Biol Chem* **280:** 8426–8434.

Voskoboinik, I., Smyth, M.J., and Trapani, J.A. (2006) Perforin-mediated target-cell death and immune homeostasis. *Nat Rev Immunol* **6:** 940–952.

Williamson, K.C. (2003) Pfs230: from malaria transmission-blocking vaccine candidate toward function. *Parasite Immunol* **25:** 351–359.

Williamson, K.C., Keister, D.B., Muratova, O., and Kaslow, D.C. (1995) Recombinant Pfs230, a *Plasmodium falciparum* gametocyte protein, induces antisera that reduce the infectivity of *Plasmodium falciparum* to mosquitoes. *Mol Biochem Parasitol* **75:** 33–42.

Wirth, C.C., and Pradel, G. (2012) Molecular mechanisms of host cell egress by malaria parasites. *Int J Med Microbiol* **302:** 172–178.

Xu, D., and Zhang, Y. (2011) Improving the physical realism and structural accuracy of protein models by a two-step atomic-level energy minimization. *Biophys J* **101:** 2525–2534.

Xu, D., and Zhang, Y. (2012) *Ab initio* protein structure assembly using continuous structure fragments and optimized knowledge-based force field. *Proteins* **80:** 1715–1735.

Supporting information

Additional Supporting Information may be found in the online version of this article at the publisher's web-site:

Fig. S1. Controls of transcript and IFA analyses.
A. RT-PCR control for possible contamination with genomic DNA. cDNA samples for trophozoites (TZ), schizonts (SZ), immature (GCII-IV) and mature (GCV) gametocytes were prepared lacking reverse transcriptase. Diagnostic PCR was performed with *pfaldolase*-specific primers and no PCR product was amplified. Arrow indicates expected size of *aldolase*-specific PCR product fragment of 378 base pairs (compare with Fig. 1B).
B. IFA control using sera from non-immunized mice for immunoblotting. Non-immunized mouse sera (NMS) were used to immunoblot fixed samples of schizonts (SZ) and mature gametocytes (mGC) (green). Schizonts were visualized by labelling with rabbit anti-MSP1 antisera and gametocytes were visualized by rabbit anti-Pfs230 antisera (red); nuclei were highlighted by Hoechst stain (blue). Bar, 5 μm.
C. Colocalization studies on PPLP2 and Pfg377. PPLP2-positive vesicles immunolabelled with mouse anti-PPLP2RP1 antisera (green) do not colocalize with Pfg377-positive osmiophilic bodies, shown using rat anti-Pfg377 antisera (red); nuclei were highlighted by Hoechst stain (blue). Bar, 2 μm. Results shown in A–C are representative for three independent experiments.
D. Fluorescence intensity measurements on labelled gametocytes. The fluorescence intensity along a longitudinal line of the gametocyte shown in C (right image) for PPLP2 (green) and Pfg377 (red) was analysed using Leica AF software.
Fig. S2. Relocalization of PPLP2-positive vesicles to the periphery of activated gametocytes is inhibited by BAPTA-AM. PPLP2-positive vesicles are present in BAPTA-AM-treated gametocytes, but do not relocalize to the periphery between 0–20 min p.a. In untreated gametocytes, PPLP2-positive vesicles relocalize upon activation and PPLP2 labelling disappears during gamete formation. Parasites were labelled with mouse anti-PPLP2RP1 antisera (green). Gametocytes were highlighted by labelling with

rabbit anti-Pfs230 antisera (red), while nuclei were stained with Hoechst (blue). Results shown are representative for two independent experiments. Bar, 5 μm.

Fig. S3. The blood stage cycle of PPLP2(–) parasites.

A. Absence of PPLP2 in PPLP2(–) schizonts. Following immunolabelling with mouse anti-PPLP2RP2 antisera, no PPLP2 signal can be detected in PPLP2(–) schizonts via IFA (green). The schizonts were visualized by rabbit anti-MSP1 antisera (red), nuclei were highlighted with Hoechst stain (blue). Results shown are representative for two independent experiments. Bar, 5 μm.

B. The morphology of PPLP2(–) asexual blood stage parasites. Giemsa smears of rings, trophozoites and schizonts were microscopically analysed and compared with WT blood stage parasites. Bar, 5 μm.

C. Kinetics of long-term asexual WT and PPLP2(–) parasite replication in human erythrocytes *in vitro*. Synchronized cultures were maintained for 7 days at 2% hematocrit. After ~ 18 h in culture parasitemia of WT and PPLP2(–) cultures was adjusted by addition of uninfected erythrocytes with the preservation of culture hematocrit. Parasitemia was assessed on days 1, 3, 5 and 7 by counting 600 to 3500 cells for each sample. A representative of four independent experiments is shown.

Fig. S4. The morphology of PPLP2(–) gametocytes and the superflagellum.

A. The morphology of PPLP2(–) gametocytes during development and following activation. Giemsa smears of gametocytes of stages I–V and of microgametocytes at 15 min p.a. were microscopically analysed and compared with WT gametocytes. Arrow indicates the superflagellum. Bar, 5 μm.

B. Immunolabelled activated PPLP2(–) microgametocyte (MiGC) forming a superflagellum. The activated microgametocyte was immunolabelled with rabbit anti-Pfs230 antisera (green), and counterstained with Evans Blue (red). The nucleus was highlighted with Hoechst stain (blue). Arrow indicates the superflagellum. Bar, 5 μm.

C. Ultrastructure of a PPLP2(–) macrogamete. Transmission electron microscopy demonstrates normal development of a PPLP2(–) macrogamete at 15 min p.a.

D. Ultrastructure of an activated PPLP2(–) microgametocyte with superflagellum. Transmission electron microscopy shows a PPLP2(–) microgametocyte at 15 min p.a., which has formed a superflagellum. The axonemes were cut longitudinally. E, erythrocyte; EC, erythrocyte cytoplasm; EM, erythrocyte membrane; IMC, inner membrane complex; N, nucleus; PDM, parasitophorous vacuole-derived membranes; PPM, parasite plasma membrane; SF, superflagellum. Bar, 1 μm.

Fig. S5. Ultrastructure of activated gametocytes chemically inhibited in egress.

A. Ultrastructure of activated microgametocytes treated with 1,10-phenanthroline. Transmission electron microscopy shows that at 20 min p.a. 1,10-phenanthroline-treated microgametocytes form superflagella containing bundles of axonemes. The superflagella were enveloped by the EM (left image modified from Sologub *et al*., 2011).

B. Ultrastructure of a gametocyte at 20 min p.a. following treatment with BAPTA-AM. The frame shown in the left image indicates the area enlarged in the right image.

C. Ultrastructure of a gametocyte at 20 min p.a. following treatment with cysteine/serine protease inhibitor TCLK.

D. Ultrastructure of a gametocyte at 20 min p.a. following treatment with cysteine inhibitor E64d. Results shown in A–D are representative for three independent experiments. Ax, axoneme; EM, erythrocyte membrane; IMC, inner membrane complex; N, nucleus; OB, osmiophilic body; PPM, parasite plasma membrane; PVM, parasitophorous vacuole membrane; SF, superflagellum. Bar, 1 μm.

Fig. S6. Effect of pore sealant on the blood stage cycle and exflagellation activity of activated PPLP2(–) gametocytes.

A. Purified recombinant full-length PPLP2. Full length PPLP2 (PPLP2RP3) was expressed in HEK-293 cells and His-tagged PPLP2RP3 was purified by Ni-NTA chromatography. SDS-PAGE followed by either silver staining or immunoblotting with anti-His antibody shows full-length PPLP2RP3 running with a molecular weight of 122 kDa as well as processing products at approximately 70 and 50 kDa.

B. Effect of Tetronic 90R4 on merozoite egress. WT and PPLP2(–) schizonts were resuspended in medium supplemented with 0.5% AlbuMax and Tetronic 90R4 in concentrations between 10–30 mg ml^{-1}, and kept for 1 h at 37°C in the environmental chambers to accumulate sites of parasite egress. Egress was assessed by light microscopy and calculated as a fraction of schizonts that finished replication cycle and released during the incubation time. A total of 300–1000 schizonts per sites of egress were counted for each experimental condition. Results are presented as mean ± SEM of three independent experiments for WT parasites. One experiment was performed with PPLP2(–) parasites to confirm Tetronic 90R4 effect on egress observed with WT parasites.

C. Motility of PPLP2(–) microgametes during a 150-min time span. The numbers of microgametocytes forming actively moving microgametes were determined between 0–150 min p.a. for 10 optical fields at 400-fold magnification.

D. Ability of activated PPLP2(–) gametocytes to form exflagellation centres after prolonged cultivation. PPLP2(–) gametocytes of the same culture were harvested at days 12 and 23 of cultivation. The numbers of exflagellation centres were quantified at 15 min (15′) p.a. for 10 optical fields at 400-fold magnification and calculated as a percentage of all actively moving microgametes (the sum of trapped microgametes and exflagellation centres were set to 100%).

Results shown in C and D represent one experiment.

Fig. S7. Genomic DNA sequence of *pplp2(–)* gene locus with positively sequenced areas for 5′ and 3′ integration of the pCAM-BSD vector construct. The homologous *pplp2* region used for generation of the gene disruption construct is highlighted in grey; the pCAM-BSD vector sequence is depicted as white letters on black background. Primers used for sequencing and the inserted stop codon are written in bold uppercase and underlined letters. Positively sequenced areas (sequences 1–4) are indicated with dotted lines underneath. Arrow heads (<; >) indicate 5′ to 3′ direction, double arrows (<<; >>) mark beginning and end of a sequence.

Movie S1. Red blood cell invasion by PPLP2(–) merozoites and transformation.

Movie S2. Egress of PPLP2(–) merozoites from infected red blood cell.

Movie S3. Influx of Alexa Fluor 488® phalloidin from the medium into an erythrocyte infected with a PPLP2(–) schizont during membrane permeabilization prior to egress.

Movie S4. Live cell recording of WT gametocyte egress from infected red blood cell in medium supplemented with fluorescent phalloidin.